2010

# BIOCHEMICAL CHARACTERIZATION OF SUPPRESSOR OF IKK-ε AND NAK-ASSOCIATED PROTEIN 1

Jonathan Forbes
*Virginia Commonwealth University*

Department of Biochemistry and Molecular Biology
Virginia Commonwealth University

This is to certify that the thesis prepared by Jonathan L. Forbes entitled "BIOCHEMICAL CHARACTERIZATION OF SUPPRESSOR OF IKK-ε AND NAK-ASSOCIATED PROTEIN 1" has been approved by his committee as satisfactory completion of the thesis requirement for the degree of Master of Science.

---

Dr. Jessica K. Bell, School of Medicine

---

Dr. Darrell Peterson, School of Medicine

---

Dr. David Williams, School of Medicine

---

[Click here and type your Committee Member's Name and School Name.]

---

Dr. Sarah Spiegel, Chair of the Department of Biochemistry & Molecular Biology

---

Dr. Jerome Strauss, Dean of the School of Medicine

---

Dr. F. Douglas Boudinot, Dean of the School of Graduate Studies

[Click here and type the Month, Day and Year this page was signed.]

# BIOCHEMICAL CHARACTERIZATION OF SUPPRESSOR OF IKK-ε AND NAK-ASSOCIATED PROTEIN 1

A thesis submitted in partial fulfillment of the requirements for the degree of Master of Science at Virginia Commonwealth University.

by

JONATHAN L. FORBES
B.A., SUNY-Buffalo, 2008

Director: DR JESSICA K. BELL
ASSISTANT PROFESSOR, DEPARTMENT OF BIOCHEMISTRY & MOLECULAR BIOLOGY

Virginia Commonwealth University
Richmond, Virginia
May 2010

Acknowledgements

I would like to take this opportunity to thank all the people who aided me in many different ways during the execution of this thesis. First and foremost, I would like to thank my mother and father. Without their support, encouragement and sagely wisdom, I might not have finished. I owe almost everything that I have accomplished in life both to their parenting and their tutelage, and from the bottom of my heart I express my deepest appreciation. I would like to thank my sister, Liz, who always had the right words to say to keep my head above water, and to keep things in perspective. I would like to thank my stepmother, Kim, and my sisters, Brooke and Shelby, who always gave me laughs, smiles and encouragement. To all of my family, thank you for being there for me and for supporting me in this endeavor.

Without the help of Dr. John Burgner, this thesis would have been infinitely more difficult. His expertise and advice on matters of analytical ultracentrifugation helped in no small part to make this thesis possible. Dr. Carlos Escalante was a gracious host in scheduling time and allowing me to use his machines to do numerous experiments. I would like to thank my committee members, Dr. David Williams and Dr. Darrell Peterson, for providing alternative paths to undertake to help characterize my constructs. I would also like to thank Dr. Celeste Powers, for providing invaluable, succinct advice and also time regarding my future endeavors.

I would like to thank the entire Bell laboratory team. Jason for providing his knowledge on the impossible proteins we work with and knowing every baseball stat since the invention of electricity, Jimmy for providing an air of lightness and professionalism to the everyday lab, Danielle for not being afraid to let things get messy during an experiment and Charlotte for her rapier like wit. Thank you all for helping me deal with the pressures and deadlines attributed to graduate school.

Last and certainly not least, I would like to thank my mentor, Dr. Jessica Bell. She is easily one of the smartest smart people I know, and I stand in awe of the knowledge she encompasses almost on a daily basis. Thank you for giving me the opportunity, financial support and lab space to evolve and execute this thesis. Without your guidance, mentoring and creative intelligence there is no question I would not have finished this thesis. Sincerely, thank you.

# Table of Contents

Page

# List of Tables

Page

# List of Figures

Page

# Abstract

BIOCHEMICAL CHARACTERIZATION OF SUPPRESSOR OF IKK-ε AND NAK-ASSOCIATED PROTEIN 1

By Jonathan L. Forbes, M.S.

A Thesis submitted in partial fulfillment of the requirements for the degree of Master of Science at Virginia Commonwealth University.

Virginia Commonwealth University, 2010

Major Director: Dr. Jessica K. Bell Ph.D.
Assistant Professor, Department of Biochemistry & Molecular Biology

Innate immunity provides the first line of defense against invading pathogen by recognizing and mounting a response to the pathogenic challenge. Among the cellular mechanisms of the innate immune response, Toll-like receptor 3 (TLR3) recognizes viral dsRNA and signals subsequent production of type-I interferon. The TLR3:interferon signaling cascades contains a kinase complex composed of two kinases and a scaffold protein, NAK-associated protein 1 (NAP1). The role of NAP1 in modulating kinase activation or regulation is unknown. A key inhibitory protein identified in the

TLR3:interferon pathway, silencer of inhibitor of κBα kinase ε (SIKE), blocks the activity of this kinase complex through an unknown mechanism. The long term goal of this project is to define how protein:protein interactions modulate signal transduction in this pathway as mediated by host in the context of an immune response, pathogen as it attempts to subvert the host immune system and in disease states such as cancer and obesity. Objectives for this thesis were to produce recombinant SIKE and NAP1 material that could be used to elucidate the self-association pattern and hetero-interactions mediated by these components within the pathway. SIKE full-length, SIKE 72 (residues 72-207), NAP 270 (residues 1-270) and NAP 255 (residues 1-255) expression constructs were completed and recombinant protein produced using either a bacterial or baculovirus/insect cell expression system. Self-association was characterized by size exclusion chromatography and analytical ultracentrifugation. Hetero-interactions were explored via co-precipitation assays of recombinant proteins. SIKE 72 formed a primarily dimeric structure whereas NAP 255 forms a single species that appears to be monomeric at this stage of analysis. Hetero-interactions form between the kinase TBK-1 and NAP 255 and also TBK-1 and SIKE 72. TBK-1 shows a higher preference for binding NAP 255 in the prescence of both NAP 255 and SIKE 72. This work provides methodology to produce recombinant material for two components of the TLR3:interferon pathway and their initial biochemical characterization for both self-association and hetero-interactions.

# Chapter 1: Introduction

## 1.1 The Innate Immune System

Innate immunity provides the first line of defense against invading pathogen. All eukaryotic organisms harbor a form of the innate immune response. This response consists of two main components: First, defend the host by sequestering the invading pathogen or danger signal by phagocytosis or release of small molecules to inhibit pathogen dissemination. Second, in higher eukaryotes, activate and modulate the adaptive immune response.

Both the innate and acquired immune systems are essential for a robust immune response in humans **[1]**. Following pathogen invasion, the innate immune system reacts within minutes to sequester the pathogen and alert the adaptive immune system, which becomes fully activated in approximately 72 hours post infection.

The innate immune response differs from acquired immunity in three aspects; First the response does not rely upon somatic recombination to produce an antigen-specific antibody but relies upon recognition of evolutionarily conserved pathogen components to activate this system. Second, the response level does not increase with redundant

exposure, but is directly correlated to tissue type and type of infection [**1**]**.** In some body tissues, an inflammatory response recruits more macrophages and dendritic cells. However, in critical organs, such as the brain or heart, inflammation can be bypassed by a macrophage response based upon phagocytosis and subsequent digestion of pathogen. Alternatively, cells can undergo controlled cell death (apoptosis) in these tissues to reduce inflammation [**1**]. Last and most importantly, the direct interaction between a bacterial or viral pathogen via a pathogen-associated molecular pattern (PAMP) with a host receptor mediates the innate immune response. Recognition of pathogen- or danger-derived substances over endogenous material separates a response beneficial to the host versus an aberrant response that can lead to numerous disease state responses [**1**].

Macrophage and dendritic cells form the backbone of the innate response, along with most epithelial cells located at mucosal barriers. Macrophages engulf foreign material, digest them internally using protein degradation enzymes and lysozymes, and release cytokines and chemokines to propagate a local inflammatory response in nearby cells [**1**]. These first responders sequester foreign cells or cellular products by phagocytosis. Dendritic cells (DCs) serve as the body's interstitial phagocytic processor by constantly sampling their environment. Immature dendritic cells reside in the periphery. Upon maturation due to external/internal exposure to cytokines or bacterial particles from phagocytosed material, they migrate to the draining lymph node, maturing as they migrate. In the lymph node, the mature DC presents the antigenic material and co-stimulatory molecule to naive lymphocytes, allowing for initiation of the acquired immune response [**1**]. In this role, DCs function as antigen presenting cells (APCs). The

ability to communicate an innate immune response to the adaptive immune system represents a critical link between the two branches of the human immune system.

Upon activation, these DCs and macrophages tailor their response to the type of infection. Similar in all responses, activated transcription factors up-regulate the production of cytokines such as interleukin-1 (IL-1), interferon (interferon-alpha (IFN-α) and interferon-beta (IFN-β)) and tumor necrosis factor-alpha (TNF-α) [**1**]. Cytokines are generally proteins, peptides or glycoproteins that are secreted to effect the processes of neighboring cells. Cytokines act in various ways to increase immune activity, from initiating maturation in dendritic cells and attracting macrophages all the way to decreasing bacterial replication and activation of the complement pathway **(Table 1).**

An example of a cytokine-mediated response is the release of interferon. Viral or bacterial challenge leads to production of interferon. Interferons are so named because they "interfere" with the replicative ability of invading pathogen [**1**]. Type-I interferons, such as IFN-α and IFN-β, act as secondary messengers of a viral infection, and mediate the activation of pathogen replication inhibitors in infected cells and also increase major histocompatibility complex molecules (MHCI and MHCII) on uninfected cells [**2**]. MHC I molecules present peptides derived from infecting pathogen for recognition by cytotoxic or helper T cells. In addition, interferon can activate natural killer (NK) cells and macrophages directly, with the net result being targeted toxicity of infected cells [**1**].

**Table 1. Cytokines and their associated function.**

| CYTOKINE | FUNCTION |
|---|---|
| **TNF-alpha** | **Local Effects**: Increases vascular system dilation, increases vascular permeability. Overall, leads to increased drainage to lymph nodes.<br>**Systemic Effects**: Increased body temperature, systemic shock. |
| **IL-6** | **Local Effects**: Activation of lymphocytes, increased production of antibodies by T-cells (Acquired Immune System).<br>**Systemic Effects**: Increased body temperature, production of acute phase proteins from hepatocytes. |
| **IL-8 (CXCL-8)** | **Local Effects**: Recruits neutrophils, basophils and T cells to site of local infection. Allows leukocytes to bind to site of infection by changing the conformation of integrin proteins. |
| **Type-1 Interferon** | **Local Effects**: Induce resistance to viral replication by activating PKR to inhibit translation, increase MHCI presentation, activate NK cells. |

A crucial level of response is required, however over-stimulation can have deleterious effects on the host. For example, bacterial infection can overwhelm a host quickly, moving beyond a localized to a systemic infection. In a systemic infection, the innate immune response can have detrimental effects on the host. When the gram-negative bacterial component, lipopolysaccharide (LPS), is recognized by the host, the host's innate immune response produces the cytokine TNF- α [**1**]. TNF-$\alpha$ functions to illicit an inflammatory response, including an increase in vascular diameter resulting in hypotension that can starve organs of necessary nutrients. [**1**]. This particular hyper-response, septic shock, results in patient death in 30-50% of the cases [**2**]. Death is nominally from bacterial infection, but directly due to the hyper-activation of the innate immune response.

Evasion of the innate immune response is just as critical an issue. If a pathogen acquires the means to either mimic or evade recognition, the step-wise dependent dynamics between the innate and acquired immune response allows for the pathogen to evade almost all types of immunological response. Numerous mechanisms have evolved in viruses to circumvent immune response. In one example, viral protein (VP35) from the Ebola virus inhibits production of interferon-$\beta$ by binding to the kinases that activate the transcription factor and acting as a competitive inhibitor for these kinases [**3**]. In a second example, Hepatitis C virus degrades and sequesters components of the viral response signaling cascade [**4**]. Finally, influenza A decreases presentation of its PAMP by sequestering its dsRNA [**4**]. These pathogens have all evolved extensive and specific mechanisms to evade an immune response.

In addition to hyper-active innate immune responses and evasion by pathogen, the innate immune system can also lose its ability to distinguish between self and non-self, targeting endogenous cells as infectious agents leading to autoimmune diseases such as Crohn's or Graves disease [**1**]. Last, but certainly not least, the innate immune response can target non-infectious agents, creating symptoms of what are commonly referred to as allergies. While seasonal allergies are generally a nuisance, allergic reactions to things such as peanuts or shellfish can be fatal and are due to the body over-reacting to a non-infectious agent [**5**].

The human body has developed an extensive, specific and highly regulated system in regard to finding and removing infectious agents. Multitudes of pathways and proteins participate in these responses. The end goal of studying the immune system is to be able to enhance the immune system's ability to recognize danger signals and to remove the danger. Enhancing the immune response may involve increasing the innate immune response and antibody production for vaccination, or to selectively inhibit pathogen silencing of an immune pathway. Alternatively, induced activation of immune response in infected tissue could help fight chronic infections or hyperplasic states. While extensive study has been put towards this avenue of research, plenty of unknowns with regard to mechanisms of action of the plethora of immune cascades associated with the innate responses remain.

### 1.2 Pattern Recognition Receptors

The cellular responses are based on differential recognition of endogenous and exogenous material, with an eye towards destroying foreign infection while leaving healthy endogenous cells intact. This delicate balance is accomplished by receptors, both intra-cellular and extra-cellular that recognize proteins and products specific to bacterial or viral processes. These recognized proteins and products are referred to as pathogen associated molecular patterns (PAMP's) [**2**]. These PAMP's, of various composition and source, are recognized by a class of protein receptors called pattern recognition receptors (PRR) [**2**]. These receptors and their consequent effect on metabolic action in various cell types allow the body to selectively respond to new or modified versions of bacterial and viral pathogens.

The structural basis of recognition of bacterial and viral particles is mediated PRRs. The patterns recognized by these receptors include LPS, double stranded RNA (dsRNA), lipoteichoic acid (LTA) from gram positive bacteria and many others, all with the common feature of being uniquely distinct from protein or molecular patterns of endogenous cells but evolutionarily conserved in pathogens [**2**].

The PRRs that recognize these PAMPs are generally classified by three expansive functions. The first class describes components that initiate phagocytosis to sequester and eliminate pathogen by immune cells such as neutrophils and macrophages. The PRRs are expressed on the cell surface, a good example being the mannose receptor (MR) [**2**]. These particular receptors recognize a distinct pattern of high mannose structures displayed on bacteria and mediate endocytosis of the associated bacteria.

The second category is the secreted PRRs, as they are secreted from cells to act on the surrounding environment. These receptors have two main functions, the first being to facilitate the complement pathway, and the opsonization of bacteria to help facilitate targeted phagocytosis by macrophages [2]. Mainly secreted by the neutrophil granulocytes and epithelial cells, defensins bind to microbial cell membrane, embed and form pore-like structures that compromise the integrity of the bacterial target [7].

The last class of PRRs is the receptors that signal the presence of infection, and they are located both extra-cellular and intracellular. Activation of signaling cascades, such as the NF-κB pathway, generally produces responses that are pro-inflammatory [2]. The major consequence of receptor activation and subsequent signaling cascades is the production of cytokines and transcription factors associated with both the innate and acquired immune response. A good example of this receptor class is the Toll-like receptor (TLR) family.

### 1.3 Toll-like Receptors

The Toll receptor was initially discovered in *Drosophila melanogaster* for its role in embryonic development **[8]**. Mutations in Toll affected dorsal/ventral patterning. Hoffman and colleagues discovered that in the adult fly, mutations in Toll compromised the fly's immunity to fungal infections [8]. Homologues of Toll were identified in humans via computational homology searches and fluorescence in situ hybridization experiments [9]. To establish a role for the human Toll-like receptors in an innate

immune response, Janeway and Medhitov ligated an antibody to a Toll-like receptor (TLR) and found activation of pathways capable of initiating an adaptive immune response [**10**]. Beutler's group further confirmed the innate immune function of human TLRs by mapping a mutation known to cause endotoxin resistance (response to gram negative bacteria) to a TLR **[11].** TLRs have since been found in organisms ranging from sea urchins to humans [**2**]. In humans, 10 TLRs are been identified which recognize ligands including lipoteichoic acid, LPS, flagellin, ssRNA, dsRNA and unmethylated CpG motifs, (**Table 2**).

As sentinels of microbial infection, human TLRs (hTLRs) are expressed on immune cells such as macrophages, mast cells, dendritic cells and natural killer cells. In addition, hTLR expression has been found in fibroblasts and keratinocytes [**12,13]** , NK [**14-16]**, and mast cells [**17,18**] as well as endothelial and epithelial cells **[19-21]**. Within a cell, TLRs can be found at the plasma membrane (TLRs 1, 2, 4, 5, 6 and 10) to directly sense potential pathogen in the extracellular milieu, or in an endosomal compartment (TLRs 3, 7, 8and 9) that samples endocytosed or autophagic components [**21**]. The external-membrane TLRs are activated by binding to mostly bacterially derived particles, such as lipopolysaccharide (LPS) from gram-negative bacteria and flagellin, the locomotive protein from flagellum-operated bacteria [**22**]. TLR localization, either plasma membrane or endosomal, allows the

**Table 2. Toll-Like Receptors and their associated adaptors.**

| TLR | LOCATION | LIGAND | CO-RECEPTOR/ADAPTOR |
|---|---|---|---|
| 1 | External Membrane | Bacterial proteins | Hetero-dimerizes with TLR2, MyD88 |
| 2 | External Membrane | PGN | MAL, MyD88 |
| 3 | Endosome | dsRNA | TRIF |
| 4 | External Membrane | LPS | MD-2, MAL, MyD88, TRAM, TRIF |
| 5 | External Membrane | Flagellin | MyD88 |
| 6 | External Membrane | Bacterial proteins | Hetero-dimerizes with TLR2, MyD88 |
| 7 | Endosome | ssRNA | MyD88 |
| 8 | Endosome | ssRNA | MyD88 |
| 9 | Endosome | CpG | MyD88 |
| 10 | External Membrane | | MyD88 |

TLRs to be directly exposed to endogenous and exogenous protein and act as a front-line detection system for the cell. The TLRs that respond to nucleic acids are all located in the endosome. This location is beneficial in multiple ways, the first being that this compartmentalization allows for intracellular infection by a virus to be detected (namely due to ssRNA and dsRNA) by normal autophagy. Alternatively, nucleic material from damaged tissues, either infected or not, can be endocytosed and initiate an immune response by creating distinctions between endogenous nucleic material and hallmarks of danger [**21**].

Structurally, the TLRs use a similar scaffold despite the variety of ligands that are capable of stimulating these receptors. TLRs are type I integral membrane glycoproteins with an N-terminal ligand binding domain consisting of a disulfide bonded capping motif, 15-24 leucine rich repeats and another disulfide bonded capping motif. The ligand-binding domain is followed by a single trans-membrane domain, which is connected to a C-terminal Toll/Interleukin 1 domain (TIR). This TIR domain connects the receptor to the cytosolic signaling pathways [**24**]. In three-dimensional space, the TLRs appear as a question mark in structure, with the "hoop" representing the ligand binding domain and the "dot" serving as the cytosolic signaling domain.

Upon ligand binding to a TLR ligand binding domain, the majority of the TLRs will either homo- or hetero-dimerize, activating a signaling cascade. TLR1 and TLR6 both hetero-dimerize with TLR2 to provide specificity for gram-positive bacterial byproducts [**23**]. More recently, it has been proposed that TLR10 interacts in some way with TLR2, however its exact ligand and activating mechanism remains unknown [**23**].

Upon TLR activation, adaptor protein binds to the cytosolic TLR-TIR through a homotypic TIR:TIR interaction. The TLRs can be divided into two classes based upon the adaptor protein used in signaling: MyD88 (myeloid differentiation factor 88)-dependent or MyD88 independent. Only TLR3 is Myd88 independent using instead the adaptor, TIR domain containing adaptor protein inducing IFN-$\beta$ (TRIF). TLR4 can utilize both MyD88 and TRIF but requires "helper" adaptors, MyD88 adaptor-like (MAL) and TRIF-related adaptor molecule (TRAM), respectively. Following adaptor docking to the receptor, depending on the TLR and signaling cascade numerous adaptors and kinase complexes are recruited with the end product being activated transcription factors that can facilitate the cellular response.

### 1.4 Toll-Like Receptor 3

Toll-like Receptor 3 (TLR3) recognizes viral genomic material, namely double-stranded RNA (dsRNA), as its PAMP. The cell has multiple sensors of this unique PAMP; TLR3, retinoic acid inducible gene-1 (RIG-I), melanoma differentiation associated gene 5 (MDA5) and dsRNA-dependent protein kinase receptor (PKR), however the action as well as localization of these 4 PRR's are different (**Figure 1**). TLR-3 is located in the endosome, whereas RIG-I, MDA-5 and PKR are located in the cytoplasm [**24**]. Although many of the activated signaling cascades of these four receptors are shared, unique aspects, such as eIF2$\alpha$ phosphorylation or involvement of

the mitochondria, indicate a multi-faceted, independently-operated response to dsRNA with built-in redundancy on a cellular level.

Stimulated TLR3 can activate the transcription factors nuclear factor-κB (NF-κB) and interferon regulatory factor 3 (IRF-3). Alternatively, TLR-3 activation can lead to cleavage of caspase 8, leading to cell death. NF-κB has been associated with the induction of a large number of pro-inflammatory chemokines, cytokines and apoptotic proteins, namely neutrophil adhesion proteins, TNF-α, IL-1 and COX-2 [**25**]. In contrast, IRF-3 phosphorylation and translocation to the nucleus is responsible, in part, for activation of IFN-β. Upon secretion, IFN-β binds to the extracellular heterodimeric receptor interferon alpha receptor 1/2 (IFNAR1/2), which, through the JAK/STAT pathways, activate interferon stimulated genes. The end effect of this interferon stimulated response is to stop protein synthesis and lead to apoptosis of virally compromised cells.

**Figure 1. Cellular sensors of double-stranded RNA.**

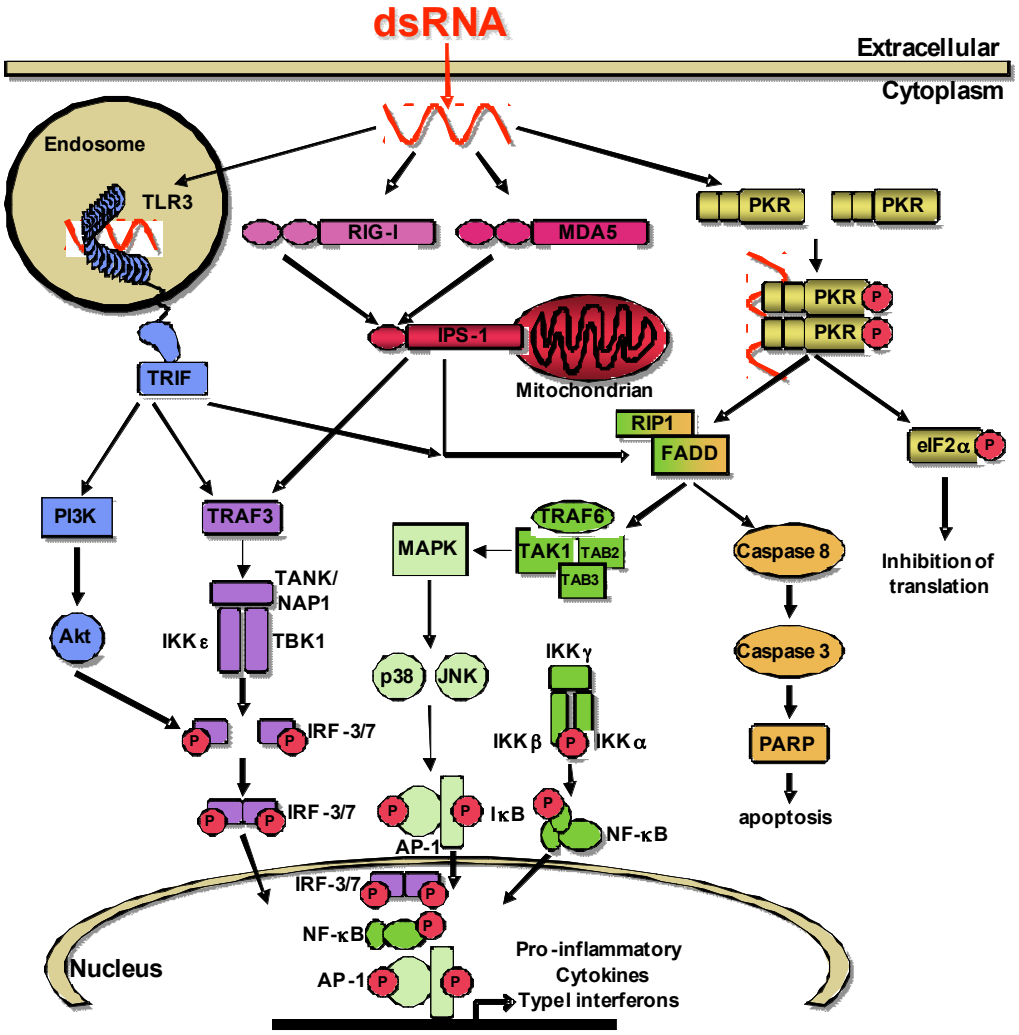


**Figure 1. Cellular sensors of double-stranded RNA.** The four intracellular receptors for double-stranded RNA and their downstream effects. RIG-1, MDA5 and PKR are distinct receptors in the cytosol, while TLR-3 is located in the endosome. Activation of these receptors leads to caspase cleavage and apoptosis or activation of transcription factor. NF-κB consists of p50 and p65, and along with IRF-3/7 serves in the activation complex for transcription of IFN-$\beta$ .

**1.5 Toll-like Receptor 3 Signaling**

The activation of TLR3 leads to four distinct responses namely cleavage of caspase 8, activation of phosphoinositide kinase-3 (PI3K) and phosphorylation and translocation of NF-κB and IRF-3 (**Figure 2**)[**24**]. As this body of work will focus upon the signaling cascade leading to IRF-3 activation, only this pathway will be described in detail. Upon ligand binding, TRIF binds to the TLR3TIR domain. TRIF, in turn, binds to its adaptor, tumor necrosis factor receptor-associated factor 3 (TRAF3), which initiates the formation of a scaffold-kinase complex. Three scaffold proteins have been identified that can function in the TLR3 signaling cascade, TRAF family member-associated NF-κB activator (TANK), NAK1-associated protein 1 (NAP1), and similar to NAP1 TBK1 adaptor (SINTBAD). Two kinases are known to associate with these scaffold proteins, TANK binding kinase 1 (TBK-1 also known as NAK) and Inhibitor of κB kinase epsilon (IKKε). Once activated, these kinases phosphorylate the transcription factor IRF-3, that can then dimerize and translocate into the nucleus, leading to the production of type I interferon (**Figure 2**).

Within the TLR-3/IRF-3 pathway, the function of the scaffold proteins associated with the kinases must be addressed for their effect on pathway activation. A scaffold protein can be loosely defined as a protein that contains a binding site for at least two other signaling proteins. *In vivo*, a scaffold protein may function as a platform for signaling molecule assembly, to localize signaling molecules, to coordinate positive or

**Figure 2. Signaling Cascades of TLR-3.**

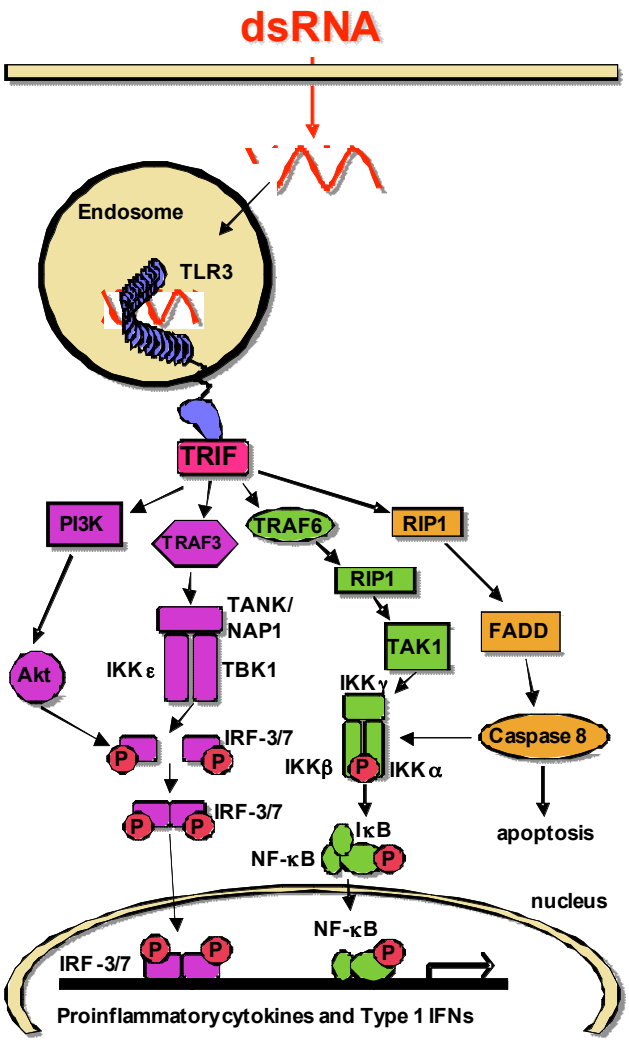


**Figure 2. Signaling Cascades of TLR-3.**TLR-3 activation leads to four distinct pathways, leading to three downstream effects. TRIF binding to the cytosolic TIR region leads to activation of Phosphoinositide-3 Kinase (PI3K), TRAF3, TRAF6 and Retinoic Inducible RIPI. A scaffold:kinase complex involving SINTBAD, NAP1, TANK and TBK1 and IKKε leads to phosphorylation of IRF3. PI3K acts by phosphorylating Akt. Subsequent signaling cascades leads to translocation of phosphorylated IRF3 and NF-kB to the nucleus and binding to interferon stimulatory response element (ISRE), to act as part of the transcription activation complex for production of type-1 interferon. TRIF binding to RIP1 leads to activation

of FADD, which assembles pro-Caspase 8 activating Caspase 8 to cleave itself to the active form and apoptotic events.

negative feedback signals or to protect activated signaling molecules from inactivation [**26**]. TANK, the most studied of the three scaffolds, is implicated in the TLR3/NF-κB pathway but may also have links to IRF-3/7 activation [**27**]. Gatot *et al.* have shown that TANK can be phosphorylated by TBK1/IKKε and that in response to pathway stimulation TANK undergoes K-63 linked ubiquitinylation. What effect phosphorylation or ubiquitinylation have on either TANK or pathway function has not yet been described. NAP1 was first identified using a yeast 2-hybrid system with TBK1 acting as the bait [**28**]. NAP1 is 392 amino acids in length, and it exhibits 28% sequence similarity to TANK. NAP1 has been shown to be the point of convergence for the TLR3 and RIG-I/mda5 pathways in the activation of IRF-3 and its knockdown could inhibit IRF-3 activation [**29**]. Co-immunoprecipitation experiments have shown that NAP1 and TBK1 complex, while NAP1 does not complex with other IKK isoforms, IKKα or IKKβ [**28**]. How NAP1 functions to activate TBK1/IKKε is not known but Fuijita *et al*. suggest that NAP1 may assist in assembly of multiple kinase units. SINTBAD, the most recently discovered scaffold of TBK1/IKKε, also functions in the TLR3/IRF-3 pathway and may form a weak interaction with NAP1 [**30**]. By comparing all three scaffold proteins, a conserved TBK1/IKKε binding domain sequence was identified and experimentally verified [**30**]. Compiled together, previous work has shown that scaffold proteins contribute to the activation of the TLR3/IRF-3 pathway, however how they may activate or modulate kinase activity remains unknown.

In the enzymatic reactions carried out during normal cellular processes, activation and inhibition of pathways must be coupled to allow a cell to respond to environmental

cues but also resolve this response to basal activation levels. Loss of cellular regulation underlies conditions such as chronic inflammation and their related diseases such as Crohn's disease, rheumatoid arthritics or atherosclerosis [**2**]. It is equally important to understand both the positive activation and negative regulation of inflammatory pathways.

Negative control of the TLR3/IRF-3 pathway is managed by at least three different regulators; A20, Src homology 2 domain-containing protein tyrosine phosphatase (SHP-2) and suppressor of IKKε (SIKE)[**31**]. A20 has ubiquitin ligase and de-ubiquitinylation activity, however, this activity does not seem to be required for TLR3/IRF-3 inhibition [**24**]. A20 co-immunoprecipitates with TRIF and TBK1/IKKε suggesting alternate mechanisms are inhibiting this pathway [**32**]. SHP-2 is a tyrosine phosphatase associated with positive regulation of cytokines such as EGF [**33**] and negative regulation of STAT1 [**34**]. In the TLR3/IRF-3 pathway, the C-terminal region of SHP-2 associates with the kinase domain of TBK1 blocking IRF-3 phosphorylation [**35**]. Both A20 and SHP-2 are not exclusive to the TLR3/IRF-3 pathway but can also regulate NF-κB activation. SIKE exclusively inhibits the TLR3/IRF-3 pathway [**31**].

SIKE was first identified in a yeast two-hybrid system using IKKε as bait and a human B-cell cDNA library [**31**]. Over expression of SIKE reduced IFN-$\beta$ production but not activation of NF-κB suggesting that this protein targets only the TLR3/IRF-3 signaling axis [**31**]. Using SIKE and either IKKε or TBK1 transfected cells, SIKE was shown to co-immunoprecipitate with both IKKε and TBK-1 [**31**]. In a resting cell, SIKE

associates with either kinase, but upon viral infection or dsRNA challenge SIKE is released from the kinases. Although the exact mechanism of inhibition has not been resolved, clearly association of SIKE with either kinase inhibits activation of IRF-3.

The TLR-3/IRF-3 pathway is one of the many viral infection response pathways the body has. Selective activation leads to production of type-1 interferon leading to immune response. The importance of this particular cascade is easily identifiable in that numerous receptors can initiate its activation. The positive impact of IFN-$\beta$ has been amply demonstrated, and recent research has shown that this cytokine could be immensely important in future cancer treatment [**36**]. Full understanding of the TLR-3/IRF-3 pathway and how to either initiate selective activation or to abolish inhibition could lead to more effective treatment regimens. Second, this pathway involves scaffold proteins, the function of which are not well understood. Gaining insight into these protein interaction networks (PINs) will help advance the field of signal transduction and increasing the overall understanding of complex PINs utilizing similar scaffolds in other pathways. Finally, understanding of the native inhibition of this pathway by SIKE could lead to better understanding of how pathogens target this particular signaling event for silencing.

This thesis was planned, executed and written with the purpose of further elucidating how SIKE and NAP1 function in the TLR3/IRF-3 pathway to regulate and activate this signaling cascade, respectively. First and foremost, how these two proteins interact in a homologous state and heterologous state within the kinase complex of the

pathway must be elucidated. Second, study how these proteins directly modulate the kinetic parameters of TBK1 and IKKε phosphorylation of IRF-3 *in vitro*.

# Chapter 2. Materials and Methods

## 2.1. Bacterial Expression Constructs and Expression

Constructs for suppressor of IKK-ε (SIKE) full length and residues 72-207 and NAK associated protein 1 (NAP1) residues 1-270 and 1-255 in the pET15b expression vector (Novagen) had previously been made. The pET15b vector, containing an ampicillin selection marker, incorporates a 6X histidine tag followed by a thrombin cleavage site N-terminal to the multiple cloning site. For expression, the plasmid of interest was transformed into BL-21 DE3 Codon + RIPL (Stratagene) competent cells following the manufacturer's protocol. A 50 ml Lennox Broth (LB) plus 100 μg/ml ampicillin was inoculated with a single colony of transformed bacteria and grown overnight at 37°C, 200 rpm in an orbital shaker. Typically 2 – 1L LB/amp cultures were inoculated with 10ml of the overnight culture and grown at 37°C, 200 rpm until $A_{600}$ reached 0.6-1 absorbance units. Cultures were then induced with 1mM isopropyl β-D-1-thiogalactopyranoside (IPTG) final concentration and grown for 4 hours at 37°C, 200 rpm. Cells were harvested by centrifugation, 8000 rpm for 20 minutes. Cell pellets were stored at -80°C.

## 2.2.Purification and Refolding of Bacterial Constructs

Cell pellet of target protein expression was resuspended in 6 M guanidine hydrochloride, 100 mM sodium phosphate, pH 8, 100 mM Tris-HCl, pH 8, 1 mM BME (Buffer 1), 5 ml of buffer 1/g of cell pellet. Resuspension was stirred at room temperature for 1 hour to solubilize all material. Homogenate was centrifuged at 12,000 rpm for 30 minutes at 4 °C. Supernatant (cell lysate) was transferred to 50 ml tubes containing Nickel-NTA agarose resin (10 ml - Qiagen), pre-equilibrated in Buffer 1. Samples of both pellet and lysate fractions were prepared for later analysis by SDS-PAGE. The lysate-resin mixture was rocked at room temperature for 90 minutes. The lysate-resin mixture was then loaded into a 250 ml Econo-Column® (Biorad). Flow through was drained by gravity and collected on ice. Resin was washed with 20 column volumes (CV) of Buffer 1. Buffer 1 wash was collected on ice. For refolding, a reverse gradient generator was set up with 10 CVs of Buffer 1 in the inner chamber, and 10 CVs of Buffer 2 (Buffer 1 sans guanidinium hydrochloride) in the outer chamber. Gradient flow through was collected on ice. Resin was washed with 2.5 CVs of Buffer 2 following the reverse gradient. Protein was eluted off the resin with 5 CVs of Buffer 3 (Buffer 2 plus 500mM Imidazole). Elution fractions were collected on ice. Samples of elution fractions were screened for target protein by SDS-PAGE analysis and visualized with coomassie blue stain.

## 2.3 Baculovirus Expression Constructs

### 2.3.1 pFastbac Construct Preparation

Constructs of SIKE and SIKE72-207 were amplified from their respective pET15b constructs using standard polymerase chain reaction (PCR) protocol. Primers incorporated unique restriction sites (5'SpeI or BamHI and 3' XhoI or SpeI for SIKE and SIKE72-207, respectively) contained in the pFASTBac vector multiple cloning site. Following amplification, the PCR product was purified using the Qiagen PCR purification kit as per manufacturer's protocol. Purified PCR product and pFASTBac vector were digested with SpeI and XhoI, or BamHI and SpeI for SIKE and SIKE72-207, respectively, for 2 hours at 37 °C. After the first hour, calf intestinal phosphatase was added to vector digest reaction. Restriction enzyme digest products were separated on a 1% agarose gel. Bands corresponding to target gene and vector were excised and gel extracted (Qiagen gel extraction kit) as per manufacturer's protocol. Vector and target gene insert were ligated in a 1:3 ratio, respectively, using a Quick ligation kit (Roche) as per manufacturer's protocol. Ligated samples and controls (vector only) were transformed into α-gold competent bacterial cells (Bioline) as per manufacturer's protocol. SIKE pFASTBac and SIKE72-207 pFASTBac colonies were amplified in 5ml LB + 100 μg/ml ampicillin. Plasmid DNA was isolated from the culture using a QIAprep spin mini-prep kit (Qiagen) as per manufacturer's protocol. DNA was eluted with sterile water. Confirmation of gene insert was achieved using a restriction enzyme digest. Plasmids containing insert were further confirmed by DNA sequencing.

### 2.3.2 Bacmid Generation

Verified SIKE pFastbac or SIKE72-207 pFastbac DNA was transformed into DH10Bac competent cells (Invitrogen). Briefly, DH10Bac cells were thawed on ice, 1 ng of pFASTBac DNA was added and mixed into 100 μl of cells in a round bottom tube. Cells were incubated on ice for 30 minutes, heat shocked at 42°C for 30 seconds, and returned to ice for 2 minutes. S.O.C. media (900 μl) was added to cells, and cells were incubated at 37°C, 200 rpm for 4 hours. After the incubation period, 250 μl cells were plated onto Lennox Broth agar plates that had been pre-treated with 100 μg/ml ampicillin, 50 μg/ml kanamycin, 7 μg/ml gentamicin, 10 μg/ml tetracycline, 40 μg/ml IPTG and 100 μg/ml X-gal in DMSO. Plates were incubated at 37°C for approximately 48 hours. White colonies were re-streaked onto Lennox Broth agar plates that had been pre-treated with 100 μg/ml ampicillin, 50 μg/ml kanamycin, 7 μg/ml gentamicin, 10 μg/ml tetracycline, 40 μg/ml IPTG and 100 μg/ml X-gal in DMSO and incubated for 24 hours. White colonies were used to inoculate 2ml LB cultures containing 100 μg/ml ampicillin, 50 μg/ml kanamycin, 7 μg/ml gentamicin, 10 μg/ml tetracycline.

### 2.3.3. Bacmid DNA Purification

Overnight cultures of pFASTBac transfected DH10Bac cells were pelleted at 9000 *xg* for 15 minutes at room temperature. Supernatant was removed, and pellet was

resuspended in 300 µl of Buffer P1 (Qiagen mini-prep kit). Cells were lysed using 300 µl of Buffer P2 (Qiagen mini-prep kit). Lysis reaction was incubated at room temperature for 5 minutes. 300 µl of 3 M potassium acetate, pH 5.5 was added drop wise with stirring, Care was taken when mixing to avoid shearing. Solution was placed on ice for 10 minutes, and then centrifuged at 14,000 rpm for 10 minutes at 4°C. Supernatant was transferred to pre-chilled microcentrifuge tube containing 800 µl of isopropanol. Tubes were stored at -20°C overnight. Tubes were spun at 14,000 rpm for 15 minutes at 4°C. Supernatant was removed. Pellet was resuspended by stirring in 1 ml of ice cold 100% ethanol. Samples were spun at 14,000 xg for 5 minutes at room temperature. Supernatant was removed. To the pellet, 50 µl of 1X Tris-EDTA buffer was layered on top followed by stirring. The bacmid solution was placed on ice for 20 minutes to allow all DNA to come into solution. Purified DNA was screened and verified by PCR. Primers used were the M13F primer (5') unique to the DH10Bac generated bacmid DNA, and a 3' primer internal to the target gene. PCR reaction and cycles were designed as per manufacturer's protocol (Invitrogen).

### 2.3.4. Insect Cell Virus Propagation

All insect cell work was carried out using sterile technique in a laminar flow hood, biosafety cabinet IIA. Sf-9 cells were cultured in Hyclone® SF-X Media (Thermo Scientific). For bacmid transfection, Sf-9s were plated in 6-well culture plates at a density of $9x10^5$ cells/well. Cells were allowed to adhere at room temperature for 1 hour. Transfection reaction was done as per manufacturer's protocol. Briefly, in a 15 ml tube, 36

μl room temperature Cellfectin® (Invitrogen) was added dropwise to 600 μl of media. Care was taken not to touch sides of the tube when adding reagent. In a separate microcentrifuge tube, 6 μg of bacmid DNA of target pFASTBac construct (SIKE FL or SIKE72-207) was added to 600 μl of SF-X media and mixed by inversion. Cellfectin® and DNA solutions were incubated at room temperature for 5 minutes. DNA solution was then added drop wise to center of the Cellfectin® solution. This Cellfectin/bacmid transfection mix was allowed to incubate at room temperature for 30 minutes. Following incubation, 4.8 ml of SF-X media was added to the transfection solution without mixing. To each well, 1ml of transfection solution was added drop wise to the center. Transfection solution incubated on cells at 27°C for 5 hours. Following incubation, transfection solution was removed and discarded, and 2 ml of SF-X media was added to each well. Cell culture plates were then transferred to a 27°C incubator. Cell morphology was observed at 24 and 48 hours for signs of cell lysis, indicating viral replication, compared to control, no bacmid DNA. At 72 hours, media from each plate was harvested and pooled. Fetal bovine serum (FBS) was added to P1 viral stock to a final concentration of 3 % of volume, to protect from protease degradation. Virus was stored at 4°C, protected from light. Amplification of a P2 viral stock was made assuming a P1 viral titer of $1x10^7$ pfu/ml. Sf-9 cultures in suspension ($2x10^6$ cells/ml) were infected at a multiplicity of infection (M.O.I) of 0.1.

$$\textbf{Inoculum Required (ml)} = \frac{\text{M.O.I (pfu/ml) (total \# of cells)}}{\text{Viral Titer (pfu/ml)}}.$$

P2 virus was harvested when cell death was >85%, approximately 80 hours post infection. To harvest virus, cells were spun down at 1,000 rpm. Supernatant was transferred to a new sterile tube, 3% FBS was added and solution was sterile filtered (0.22 μm filter). P2 virus was stored at 4°C, protected from light.

### 2.3.5. Determining Viral Titer

Plaquing assay to determine viral titer was completed as per Bac-to-Bac® instruction manual (Invitrogen). Briefly, Sf-9 cells were plated at a density of 1.0 x $10^6$ cells/well in two 6-well culture plates. Cells were adhered at room temperature for 1 hour. Serial dilutions of P2 viral stock were made from $10^{-1}$ to $10^{-7}$ fold dilutions in SFX media. Media was removed from cells and replaced with 1 ml of diluted virus. Each dilution of virus was done in duplicate, along with a control (no viral addition). Wells were allowed to incubate with virus for 4 hours at room temperature on an orbital shaker, slow speed. Low melting temperature agarose (4 %, 10 ml) and 30 ml of SF-X media were warmed to 37°C, and then combined to make plaquing media. After incubation, plates were returned to hood, and plaquing media was allowed to cool but not thicken to prevent cell death. Viral dilution media was removed from cells, and 2ml of plaquing media (cooled slightly) was added to wells, slow addition along the wall of the well. Plaquing media was allowed to set for 20 minutes with the lid slightly cracked to avoid condensation. Plates were placed in a humidified incubator at 27°C for 4 days. To stain for plaques, 1 ml neutral red staining solution, consisting of 1% agarose, 62.5 μg/ml neutral red stain in SFX media, was added

to each well. Agarose was allowed to harden and plates were returned to humidified incubator for 2-3 days. Plaques (cleared areas) were counted for each well, and averaged for each dilution. Titer was calculated by:

**Titer (pfu/ml)** = (# of plaques) x (dilution factor) x (1ml of inoculum/well)

Viral stocks were replenished using the protocol described for P2 viral stock and titred as described above.

### 2.3.6. Baculovirus Expression and Protein Purification

For small-scale trial expression, Sf-9 cells were plated in 6-well plates at a density of 2 x $10^6$ cells/well. Cells were infected with a viral volume calculated as follows:

$$\textbf{Inoculum Required (ml)} = \frac{\text{M.O.I (pfu/ml) (total \# of cells)}}{\text{Viral Titer (pfu/ml)}}.$$

using an M.O.I of 3. Cells were harvested after 48 and 72 hours by washing cells from well by repeated pipetting. Cells were pelleted at 10,000 rpm for 3 minutes. Resulting pellets were resuspended in 500 μl of 1X PBS. To lyse, cells were sonicated on ice for 20 seconds. Resulting homogenate was centrifuged at 14,000 rpm at 4°C for 10 minutes. Supernatant (soluble protein) was transferred to a new tube. Pellet (insoluble protein) was resuspended in 1X PBS. Samples were analyzed by SDS-PAGE to determine solubility of target protein expression.

For large scale insect cell-derived protein production, 2 L of cell suspension were infected as above. Cells were pelleted 62 hours post infection by centrifugation at 8,000 rpm for 20 minutes. Resulting pellet was resuspended in FLAG®-wash buffer (50 mM Tris-HCl, pH 8, 250 mM NaCl, 0.5 mM NaF, 0.1% tween20, 10% glycerol, 1 tablet of EDTA-free Complete Protease Inhibitor (Roche)) at a ratio of 15ml buffer:1g pellet. Cells were emulsified (Avestin Emulsifex C3) as per manufacturer's protocol (average psi ~15,000). Resulting homogenate was spun at 12,000 rpm for 30 minutes at 4°C. Supernatant was transferred to a tube containing 15ml of FLAG® M2-agarose affinity gel (Sigma-Aldrich) pre-equilibrated in FLAG® wash buffer, and supernatant/agarose FLAG® was loaded onto an Econo®-column (250 ml volume, BioRad) and allowed to drain by gravity. Resin was washed with 20 column volumes of FLAG®-wash Buffer. Target protein was eluted with five 10 ml volumes of FLAG®-wash buffer plus 0.34 mg/ml FLAG® peptide (Sigma-Aldrich). Resin was regenerated and stored as per manufacturer's protocol (Sigma-Aldrich). Samples from each step were analyzed by SDS-PAGE. Elution fractions containing target protein were pooled and stored at 4°C. To remove FLAG® peptide from target protein, samples were separated on a Superdex™ 200 column (GE Healthcare) as described under the Size Exclusion Chromatography section.

**2.4. Mammalian Cell Transfection Construct Preparation**

Constructs of TBK-1, NAP1, TANK and SIKE 1-207 were amplified from their respective constructs (pET15b-SIKE, pUNO-TBK1, pET15bNAP1 and pET15bTANK)

using standard polymerase chain reaction (PCR) protocol. Primers were designed to incorporate restriction digest sites exclusive to the pCMV-Vector multiple cloning site. Following amplification, the PCR product was purified using the Qiagen PCR purification kit per manufacturer's protocol. Purified PCR product and pCMV vector incorporating either a Myc®-tag or a HA®-tag were digested with Not1 and SalI for 2 hours at 37 °C. After the first hour, calf intestinal phosphatase was added to vector digest reaction. Restriction enzyme digest products were separated on a 1% agarose gel. Bands corresponding to target gene and vector were excised and gel extracted (Qiagen gel extraction kit) per manufacturer's protocol. Vector and target gene insert were ligated in a 1:3 ratio, respectively, using a Quick Ligation kit (Roche) per manufacturer's protocol. Ligated samples and controls (vector only) were transformed into α-gold competent bacterial cells (Bioline) as per manufacturer's protocol. Colonies were inoculated in 5ml LB + 100 μg/ml ampicillin. Plasmid DNA was isolated from the culture using a QIAprep spin mini-prep kit (Qiagen) as per manufacturer's protocol. DNA was eluted with sterile water. Confirmation of gene insert was achieved using a restriction enzyme digest. Plasmids containing insert were further confirmed by DNA sequencing and transformed into α-bronze competent bacterial cells (Bioline) as per manufacturer's protocol. A single colony was used to inoculate 100 ml LB + 100 μg/ml ampicillin. Plasmid DNA was purified using an EndoFree® Plasmid Maxi kit (Qiagen) per manufacturer's protocol.

**2.5 Size Exclusion Chromatography**

Elutions from Ni-NTA purification and FLAG® purification were separated on a Superdex™ 200 16/60 prep grade column (GE Healthcare) pre-equilibrated in 20 mM HEPES, pH 7.5, 500 mM NaCl, 5% glycerol and 1 mM DTT (Buffer 4). Elution volumes at peak maximums were converted to $K_{av}$ and compared to a standard curve ($K_{av}$ versus log molecular weight) based upon globular standards of known molecular weights (previously derived) using the equation:

$$K_{av} = \frac{\text{elution volume} - \text{void volume}}{\text{total volume} - \text{void volume}}$$

Peak fractions for all runs were analyzed by 10% SDS-PAGE and visualized with coomassie blue stain.

**2.6 Complexing Interactions Using Size Exclusion Chromatography**

TBK-1 frozen stock protein in 50 mM TRIS pH 8, 500 mM NaCl, 0.5 mM EDTA, 0.05% TritonX-100, 2mM DTT and 50% glycerol (Freezing buffer) was defrosted on ice, and mixed in a 1:1 molar ratio with pooled NAP 270 (1 μM). Samples of TBK1 and NAP1-270 alone were prepared at 1 μM to run as controls. All samples were incubated at 4°C overnight. Samples were loaded onto a GE Healthcare Superose™ 6 10/300 Tricorn™ column. Samples were run in Buffer 4. NAP 255 and TBK-1 were complexed as above, except that TBK1 was a fresh preparation, not frozen. Samples were mixed in a 1:1 molar ratio (1.8 μM). Peak fractions from all separations were analyzed by SDS-PAGE and visualized with coomassie blue stain, followed by silver staining.

## 2.7 Circular Dichroism and Thermal Melt

NAP 255 and NAP 270 target protein samples were dialyzed into 50 mM sodium phosphate, pH 8, 50 mM sodium chloride overnight at 4°C. Dialysis buffer was retained as a buffer blank. Aggregate was removed by centrifugation, and resulting protein solution was diluted until $A_{222nm} \leq 1.0$. Spectra (190-300nm) were collected on a Jasco 720 Circular Dichroism Spectrometer via collaboration with Dr. Ellis Bell at the University of Richmond. Five individual spectra were collected, averaged and smoothed using the Jasco Spectra Manager software. Thermal melt data were collected from 4°C-90°C at $A_{222nm}$. Data were smoothed using the Jasco Spectra Manager software.

## 2.8 Analytical Ultracentrifugation

Target protein samples were concentrated to an $A_{280nm}$ of 1.0. Sample was dialyzed into 20 mM HEPES, pH 7.5, 250 mM sodium chloride and 5% glycerol overnight using Spectra/Por® 7 dialysis membrane, 10,000 MWCO (Spectrum) at 4°C covered with parafilm to prevent evaporation. Dialysis buffer was saved (50ml) in an airtight tube immediately upon recovery. Target protein was recovered and spun down at 4,000 rpm for 7 minutes at 4°C. Supernatant was removed, and its $A_{280nm}$ was recorded. Sample was used to run a sedimentation velocity experiment. Protein was loaded (410 μl) into sapphire window cells. Data were collected using a Beckman-Coulter Optima XL-A analytical ultracentrifuge (Beckman-Coulter) with an An-60 Ti rotor at 4°C. Runs for NAP 255 were

collected (9.2 μM and 18.7 μM) in duplicate. Runs of SIKE 72-207 were collected (4.2 μM). Data were analyzed using SEDFIT [**46**] program. Solvent density and partial specific volume were calculated using SEDNTERP program [**46**].

**2.9 Protein Co-precipitation**

Experiments were designed to utilize 10 μg of defrosted TBK-1, and 25 μg of either NAP 255 or SIKE 72 purified and pooled from SEC in Buffer 4. Proteins alone (controls) or mixed with potential interacting partners were incubated on ice for 1 hour prior to dilution in cold Buffer 4 to a final volume of 1ml. FLAG®M2-agarose affinity gel, previously equilibrated in 1X TBS and then Buffer 4 on ice, was added to each reaction tube (20 μl of resin). A buffer control plus resin was included in each experiment. Reactions were incubated with resin overnight at 4°C on an orbital rotator such that resin would remain suspended. After overnight incubation, resin was spun down at 4,000 rpm for 2 minutes at 4°C. Supernatant was removed, and resin was washed 3 times with 1ml of ice-cold Buffer 4. Washed resin was then resuspended in 30 μl of 2X loading dye with no reducing agent. Samples were boiled at 95°C for 3 minutes, and then placed on ice. Resin was pelleted at 4,000 rpm for 2 minutes at 4°C , and supernatant was transferred to a new tube. Two gels were ran, samples (15 μl) were separated by SDS-PAGE, transferred to a nitrocellulose membrane, which was blocked in 1X Tris-buffered saline, 0.5% Tween 20 (Buffer 6) plus 5% milk and then probed with 1:1000 dilution in Buffer 6 of antibody for 1

hour. Starting target protein (10 μg or 25 μg respectively) was also included in SDS-PAGE analysis as a reference control. Two blots were probed with either anti-Flag M2 peroxidase conjugated antibody A8592 (Sigma) or α6x-His-HRP antibody (BD Clonetech) Blots were washed 5X in Buffer 6, and and developed with standard ECL reagent (GE Healthcare) and one-fourth Dura ECL (Pierce).

**2.10 Mammalian Cell Lysate Co-Immunoprecipitations**

HEK293 cells ($3x10^5$ cells/well) were seeded in 6-well plates and transfected the following day with either Fugene® or Lipofectamine® as per manufacturer's protocol using 4 μg of target pCMV vector. 24 hours post-transfection, cells were recovered and lysed in 0.02M Tris, pH 7.5, 0.15M NaCl, 1X protease inhibitor (Complete-EDTA free Protease inhibitor tablet, Roche), 1X phospho-stop (Roche) and 1% NP40 (Buffer 5) by incubation on ice for 30 minutes, vortexed for 10 seconds every 10 minutes during incubation. Lysates were spun at 13,000 rpm for 15 minutes to pellet insoluble material. Cleared lysates were transferred to a new tube. Lysate (800 μl) was incubated with 25 μl of anti-HA antibody conjugated to agarose resin (Sigma) that was pre-equilibrated in Buffer 5 overnight on an orbital rotator at 4°C. Resin with Buffer 5 alone was included as a control. Agarose was pelleted by centrifugation and washed 3X with 1 ml Buffer 5, and layered with 40 μl of Buffer 5. Agarose was resuspended in 60 μl 2X loading dye and boiled for 3 minutes at 95 °C. Samples were spun down and supernatant was transferred to a fresh tube. Samples were separated by SDS-PAGE, transferred to a nitrocellulose membrane, which

was blocked in 1X Tris-buffered saline and 0.5% Tween 20 (Buffer 6) plus 5% milk and then probed with 1:1000 dilution in Buffer 6 of antibody for 1 hour. Antibody used was anti-HA.11 antibody (Covance) for 1 h in Buffer 6. Blot was washed 3X with Buffer 6 and probed with 1:5,000 secondary antibody, goat anti-mouse IgG conjugated to horseradish peroxidase (HRP), in Buffer 6 for 1 hour. Blot was washed 3X with Buffer 6 and developed with standard ECL reagent (GE Healthcare) and one-fourth Dura ECL (Pierce).

For further study, HEK293 cells were plated as previous, however 24 hours post-transfection with Lipofectamine with 4 μg pCMV-HA-SIKE FL cells were incubated for 24 hours or stimulated with 50 μg of pI:pC for 24 hours. Lysates were recovered and immunoprecipitated with anti-HA resin as previously described, and samples were separated by SDS-PAGE and transferred to nitrocellulose membrane. For phosphoserine screening, SDS-PAGE gel was transferred to PVDF membrane (Bio-rad), blocked in Buffer 6 with 5% BSA for 1 hour and washed 3X with Buffer 6. Antibody anti-phosphoserine 05-1000 (Upstate) was diluted 1:1000 in Buffer 6 with 5% BSA and probed for 1 hour. Blot was washed for 20 minutes 3X with Buffer 6 and probed with 1:5,000 secondary antibody, goat anti-mouse IgG conjugated to horseradish peroxidase (HRP), in Buffer 6 for 1 h. Blot was developed as previously described. For ubiquitin screening, protocol was the same as the anti-HA probe with exception of primary antibody used was anti-Ub (sc130410 Santa Cruz).

## 2.11 Crystallization Trials

SIKE 72-207 was concentrated to 6.98 mg/ml in Buffer 4. A factorial screen, Qiagen Classics Suite, was setup in a Corning® Protein Crystallography non-treated 3:1 96-well plate using 1 μl protein solution and 1 μl well solution. Plate was incubated at 18 °C and results were interpreted 2 weeks and 4 months after setup. Wells were scored as clear, precipitate, microcrystalline or crystal. A second screen was set up for SIKE 72-207 at 4.98 mg/ml using the PEGs Suite (Qiagen). Results were scored 2 weeks and 4 months after set up.

## 2.12 Protein Concentration

Protein concentrations were determined by BioRad protein assay (BioRad) as per manufacturer's protocol. As needed, protein samples were concentrated by ultrafiltration technique (Centriprep or Amicon Ultrafiltration Units, Millipore Corp.).

# Chapter 3. Results

Review of the predicted domain structure of the scaffolds, kinases and SIKE immediately suggests the potential importance of coiled-coil mediated interactions (**Figure 3**). All six proteins involved at this particular step in the cascade are predicted to have at least one coiled-coil domain. These elements can form important interactions at points of homologous and heterologous protein binding and are capable of forming dimeric up to heptameric interactions [**6**]. In this thesis, how the coiled coil domain of these kinase complex components participate in protein:protein interactions has begun to be defined.

## 3.1 Expression of Constructs

The first step in elucidating a mechanism of activation/inhibition or protein interactions *in vitro* involves production of soluble, pure and stable protein constructs. Protocols to produce recombinant kinases from insect cell culture had previously been developed and implemented (R. J. Call personal communication). Initial experiments to produce full-length (FL) SIKE in bacteria resulted in insoluble material using several bacteria cell lines and induction temperatures (R. J. Call personal communication, **Figure 4**).

**Figure 3. The Kinases, Scaffolds and Inhibitor of the TLR-3 IKKε/TBK1 Pathway**

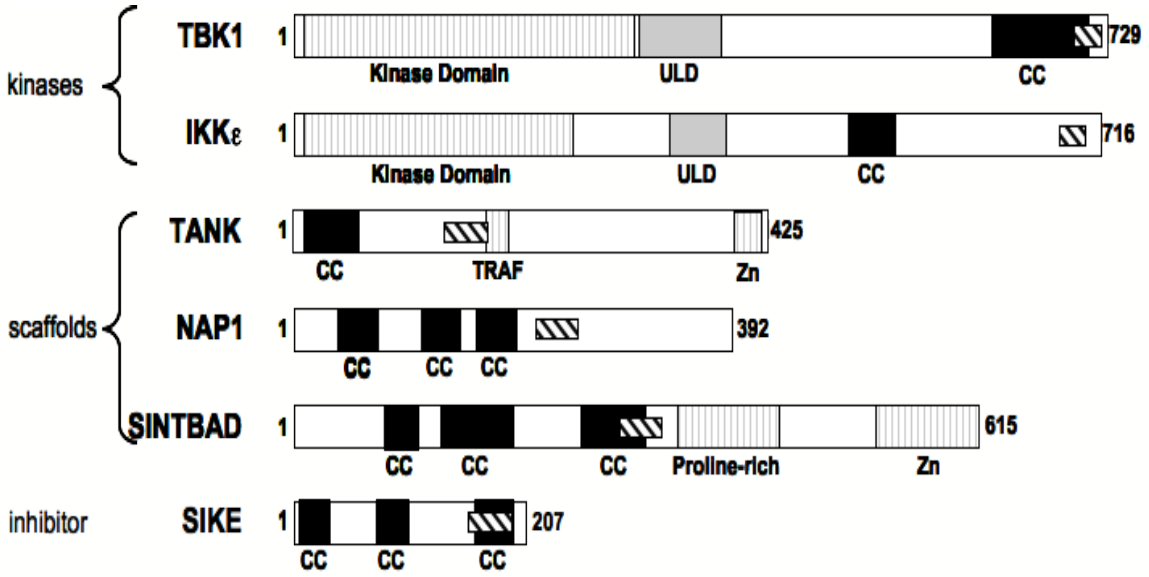


**Figure 3. The Kinases, Scaffolds and Inhibitor of the TLR-3 IKK-e/TBK-1 Pathway**

This figure diagrams the predicted domain structure of the players involved TLR-3:IKK-e/TBK-1 Pathway. Overview of the structures suggests the importance of the coiled-coil interactions for this particular pathway; predicted coiled-coil domains are depicted in black. Preliminary review of sequences has allowed for a loose prediction of Scaffold Binding Motif for the kinases, which is on the c-terminal portion and is hatched in color. The scaffolds also have their predicted Kinase Binding Domain (KBD) depicted in hatched coloring, and the inhibitor SIKE also has a predicted KBD depicted in hatched coloring. SINTBAD is another identified scaffold that was not currently under study based on its complexity.

**Figure 4. Solubility of SIKE Full Length**

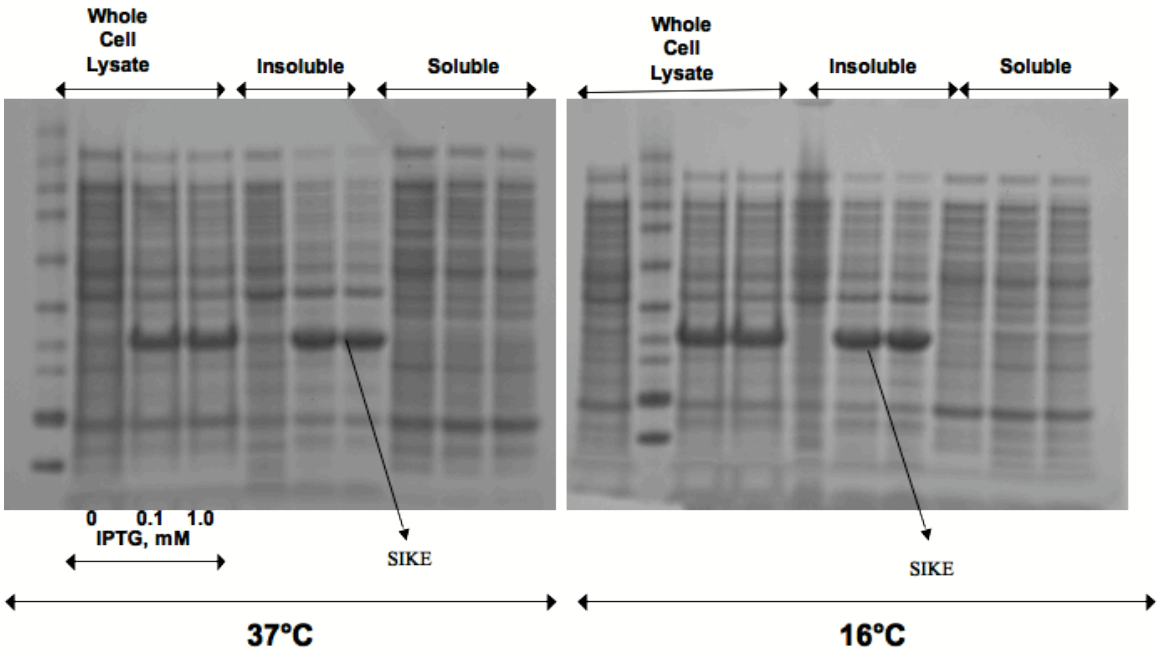


**Figure 4. Solubility of SIKE Full Length**. SIKE FL pet15b plasmid was transformed into DE3 RIPL bacterial competent cells. Cells were grown at 37 °C until $A_{600}$ = 1.0. Cultures were induced with either 0.1 mM or 1 mM IPTG. Cultures were then incubated at either 37 °C or 16 °C for 4 hours or overnight respectively. Cultures were pelleted and resuspend in 1X PBS and sonicated for 30 seconds, 3 times. Small sample of homogenate was saved (Whole Cell Lysate), the rest was centrifuged, and supernatant was transferred to a new tube representing the soluble fraction. Pellet was resuspended in water and represented the insoluble fraction. Samples were separated by SDS-PAGE. SIKE FL is insoluble.

Insoluble material was purified under denaturing conditions on an immobilized metal affinity chromatography column (IMAC) and refolded using a linear reverse gradient. Purified SIKE was analyzed by size exclusion chromatography to assess native molecular weight and oligomeric state. Separation by SEC revealed multiple species, indicating that SIKE could form multiple oligomeric states. Although known to form oligomers [**31**], SIKE's native state could not be ascertained from this experiment nor could this heterogeneous material be used to further study protein:protein interactions.

Only amino acids 72-207 of SIKE (SIKE 72) are necessary to immunoprecipitate TBK-1 and IKK-ε [**31**]**.** This shortened version, previously inserted into a pET15b expression vector, was transformed into BL21de3 cells. Again, the initial trial yielded a protein that was insoluble. Lowering induction temperature, to enhance folding, had no effect on solubility (**Figure 5**). BL21de3 Codon+ cells, which contain tRNA synthetases for *E. coli* rare codons and would enhance expression of human-derived sequences like SIKE, again, had no effect on solubility.

Based upon these difficulties with bacterial production of SIKE, an insect cell expression system was attempted for both SIKE 72 and SIKE Full Length (SIKE FL). Insect cells are more advanced on an evolutionary standpoint compared to bacterial expression systems; Insect cells have more chaperones to assist in the protein folding processes. This feature would favor producing a stable and soluble SIKE construct. To utilize insect cells for expression, the gene of a target protein must be delivered to the insect cell via a baculovirus. To produce recombinant baculovirus containing the target

**Figure 5. Solubility of SIKE 72.**

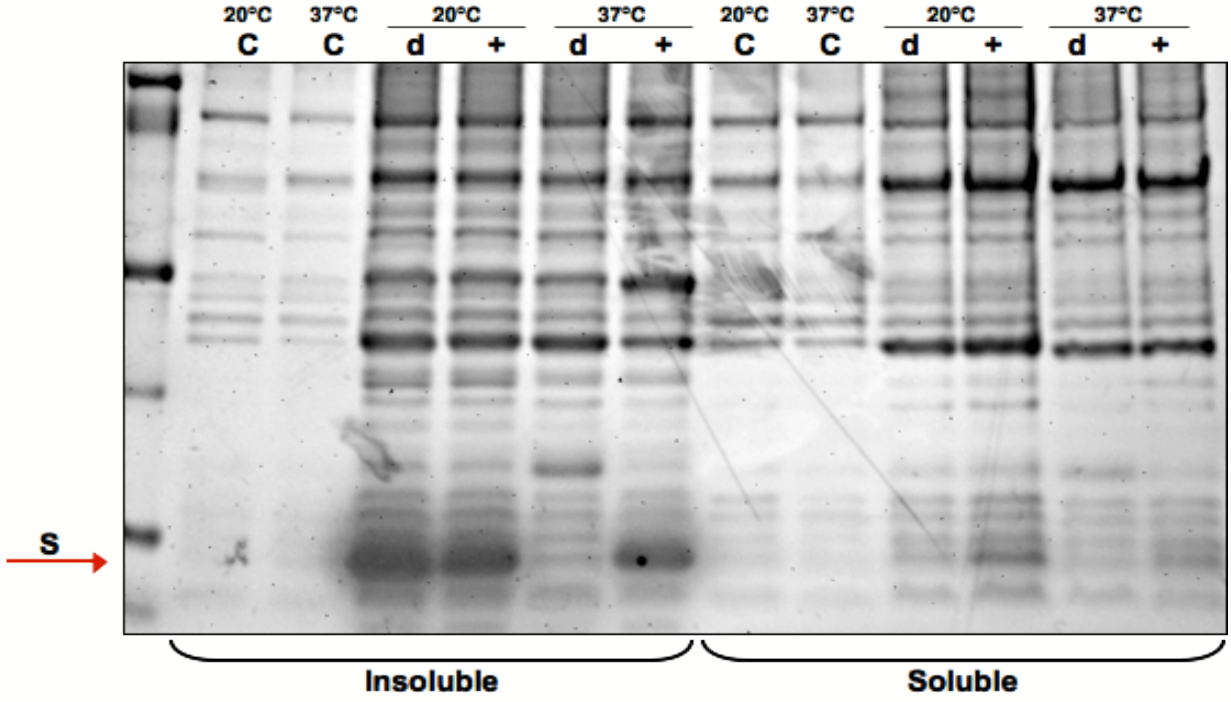


**Figure 5. Solubility of SIKE 72.** SIKE 72-pET15b plasmid was transformed into de3 RIPL bacterial competent cells. Cells were grown at 37 °C until $A_{600}$ = 1.0. Cultures were induced with either 0.1 mM or 1 mM IPTG. Cultures were then incubated at either 37 °C or 20 °C for 4 hours or overnight respectively. Cultures were pelleted and resuspend in 1X PBS and sonicated for 30 seconds, 3 times. Homogenate was centrifuged, and supernatant was transferred to a new tube representing the soluble fraction. Pellet was resuspended in water and represented the insoluble fraction. Samples were separated by SDS-PAGE. SIKE 72 is insoluble.

gene required introduction of target gene into the viral genome. . First, the gene was inserted into the pFASTBac vector, a phage shuttle vector. SIKE (FL or 72) pFASTBac was then transformed into DH10Bac competent cells, which carry the baculovirus genetic material (bacmid DNA). Through a homologous crossover event, the target gene is incorporated into the bacmid DNA. The homologous crossover has a low efficiency for producing SIKE containing-bacmid DNA. To screen for positive crossovers, colonies were selected based upon antibiotic resistance and galactosidase activity, as successful recombination should disrupt galactosidase gene product but retain antibiotic resistance. Complicating selection, colonies were mostly white upon initial growth, but often when re-streaked under the same selection would reveal galactosidase activity. Positive colonies were amplified in suspension and their DNA was isolated. Bacmid DNA isolation had numerous issues. Sensitivity to DNA shearing due to its larger size, was avoided by not pipetting to resuspend but rather using the pipette tip to gently stir solution. Even after resuspension, DNA could be compromised. Initial attempts using a Bacmid DNA Isolation kit from Invitrogen resulted in DNA pellets that were insoluble. This insolubility was coincident with allowing pellets, following ethanol precipitation and washing, to air-dry too long. Repeated attempts decreasing dry time from 10 minutes to almost 1 minute did not result in a soluble pellet. Changing the resuspension solution to either sterile water or Tris-EDTA, pH 8 buffer failed to have any effect on insoluble pellets. Pellets were also warmed in a 37°C degree water bath for 10-60 minutes but pellets remained insoluble. The final protocol that allowed for resuspension of the bacmid DNA pellet included an increased incubation on ice following resuspension in iso-propanol, and upon pelleting to

use 1ml of ice-cold ethanol and resuspend by “blasting” the pellet immediately. After spinning and pulling off ethanol, the pellet was allowed to air dry on an incline on a towel for 5 minutes. The pellet was then layered with ice cold TE Buffer and incubated on ice for 20 minutes with occasional mixing. Resuspension was incubated at 4 °C and took approximately 24 hours. The resulting bacmid DNA was screened using a standard PCR protocol with a bacmid-based 5’ primer (M13Forward) and a 3’ primer internal to the target gene (**Figure 6**). Amplification indicated insertion as well as correct orientation. Using this protocol, human Toll-like receptor 3 full-length pFASTBac and bacmid DNA were also produced, however this construct was not used in any of my further studies (data not shown).

Virus was prepared as noted in the methods. Subsequent amplification and titer quantification were completed for both SIKE FL and SIKE 72. Both viruses were amplified to a volume of 200 ml each before being titred, and the subsequent titers were as follows:

SIKE FL - $1.48 \times 10^7$ pfu/ml

SIKE 72-207 – $1.73 \times 10^7$ pfu/ml

hTLR-3 - $3.60 \times 10^7$ pfu/ml

Following viral quantification, insect cells were infected with target baculovirus in 6-well plates. Single infections of both SIKE FL and SIKE 72-207 viruses were carried out as described in the methods section. Resulting cell pellets were resuspended in 1X

**Figure 6. SIKE FL and SIKE 72 Bacmid Generation.**

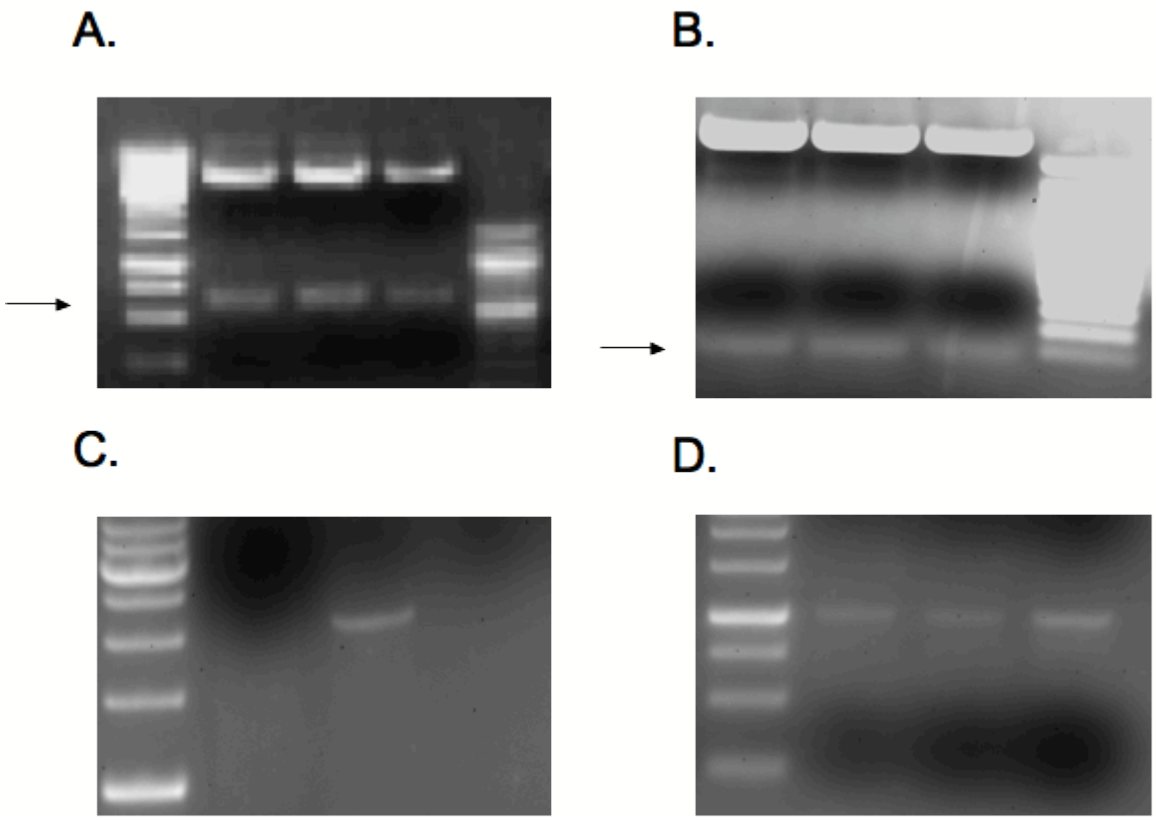


**Figure 6. SIKE FL and SIKE 72 Bacmid Generation.** The initial step of the bacmid construction was insertion of SIKE FL or SIKE 72 into a pFastbac vector. **A**.) SIKE FL restriction digest of vector shows pFastbac vector and SIKE FL DNA (arrow) **B**.) Restriction digest of vector shows pFastbac vector and SIKE 72 DNA (arrow). Due to the low concentration of vector, gel was overexposed making a marker hard to identify, however an underexposed picture was taken as well (data not shown). **C**.) PCR screen using purified SIKE FL Bacmid DNA as templates (3 in total), using an M13F primer specific for the Bacmid vector and an internal primer that sets down around residue 163 in the SIKE construct. Amplification indicates insertion as well as orientation. Only 1 of 3 samples screened was positive. **D**.) PCR screen using purified SIKE 72 Bacmid DNA as templates (3 in total), using an M13F primer and the 3' SIKE FL/72 primer used for initial amplification. Again, amplification indicates insertion as well as orientation. All 3 samples were positive.

PBS, and sonicated for 30 seconds on ice. Soluble and insoluble fractions were separated by centrifugation, prepared for SDS-PAGE analysis and separated on a 10% SDS-PAGE gel. SIKE FL and SIKE 72 are insoluble in single infections **(Figure 7).** Co-infections of SIKE FL + TBK1 virus or SIKE FL + IKKε were completed. R. J. Call provided virus for TBK1 and IKKε. Based upon the idea that SIKE bound to the kinases [**31**] and that kinases were produced as soluble proteins from insect cell culture, co-expression of SIKE + kinase would either stabilize or pull SIKE into the soluble fraction. In addition, if these proteins formed a stable complex, SIKE could be purified utilizing the kinase purification scheme. SIKE FL and SIKE 72 double infection experiments were completed, and results for both constructs were the same (**Figure 8)**. Both experiments were consistent with insoluble SIKE upon double infection . A small percentage of total SIKE expression may separate to the soluble fraction. However, a Western blot, run to confirm localization to the insoluble fraction, revealed that this construct did not contain an engineered FLAG®-tag. The incorrect pFastBac plasmid was used in the initial construct formation. However, these experiments show conclusively that SIKE FL and SIKE 72 are mostly insoluble. No further work was completed using the insoluble SIKE material from insect cells as bacteria could provide the same starting material more economically. Characterization of SIKE was exclusively on bacterially produced and refolded SIKE 72 (**Figure 9**).

The scaffold protein, NAP1, was produced exclusively in bacteria. Full length NAP1 expressed as insoluble material. Two constructs, NAP 1-270 and NAP 1-255, containing the coiled coil region and kinase interaction site, had previously been prepared.

**Figure 7. Solubility of Bacmid-derived SIKE FL**

A.

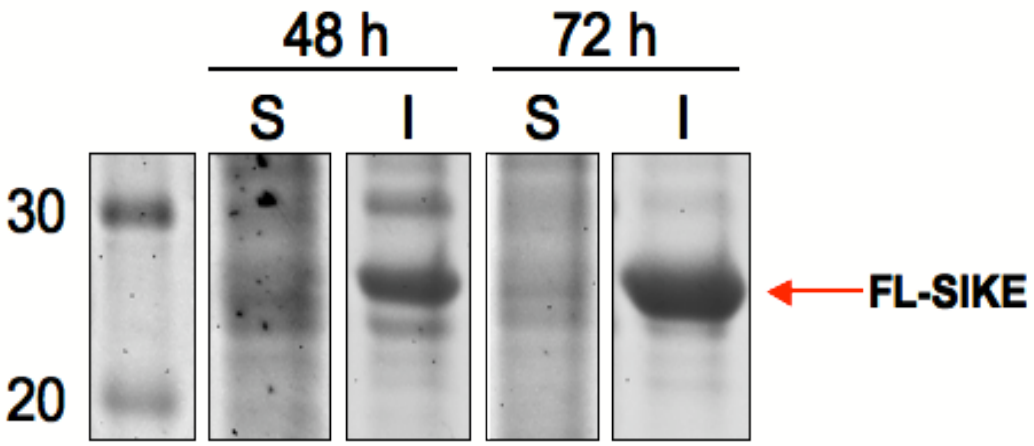


B.

**Figure 7. Solubility of Bacmid-derived SIKE FL.** Sf-9 cells in 6 well plates were infected with SIKE FL Baculovirus. Control plates had no viral infection. Cells were incubated at 27 °C and harvested at either 48 or 72 hours. Upon harvesting, cells were pelleted and resuspended in 1X PBS. Cells were sonicated and centrifuged. Supernatant was the soluble fraction, and pellet resuspended in water was the insoluble fraction. The time points and soluble and insoluble fractions (S,I) are shown. SIKE FL, upon infection, is insoluble. Repeated experiment on SIKE 72 Baculovirus was consistent with this result (data not shown).

**Figure 8. Double Infections of Bacmid TBK1, IKKε and SIKE FL.**

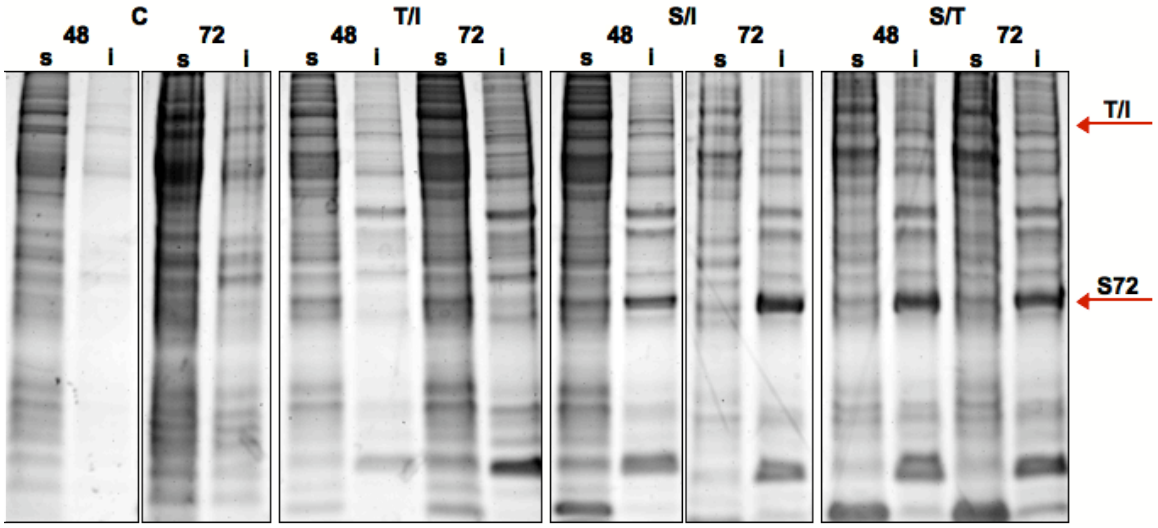


**Figure 8. Double Infections of Bacmid TBK1, IKKε and SIKE FL.** Sf-9 cells in 6 well plates were infected with SIKE FL Baculovirus along with either TBK1 or IKKε Baculovirus. Control plates had no viral infection. Cells were incubated at 27 °C and harvested at either 48 or 72 hours. Upon harvesting, cells were pelleted and resuspended in 1X PBS. Cells were sonicated and centrifuged. Supernatant was the soluble fraction, and pellet resuspended in water was the insoluble fraction. Infections (TBK1+SIKE (S/T), IKKε +SIKE (S/I) and TBK-1+IKKε (T/I)), their time points and soluble and insoluble fractions (S, I) are shown. SIKE FL, upon double infection, is insoluble, and SIKE 72 Baculovirus was consistent with this result (data not shown). While there might be a small portion of SIKE in the soluble portion, majority of SIKE is insoluble.

**Figure 9. Refolding of SIKE 72-207 From BL-21 Codon+ Expression.**

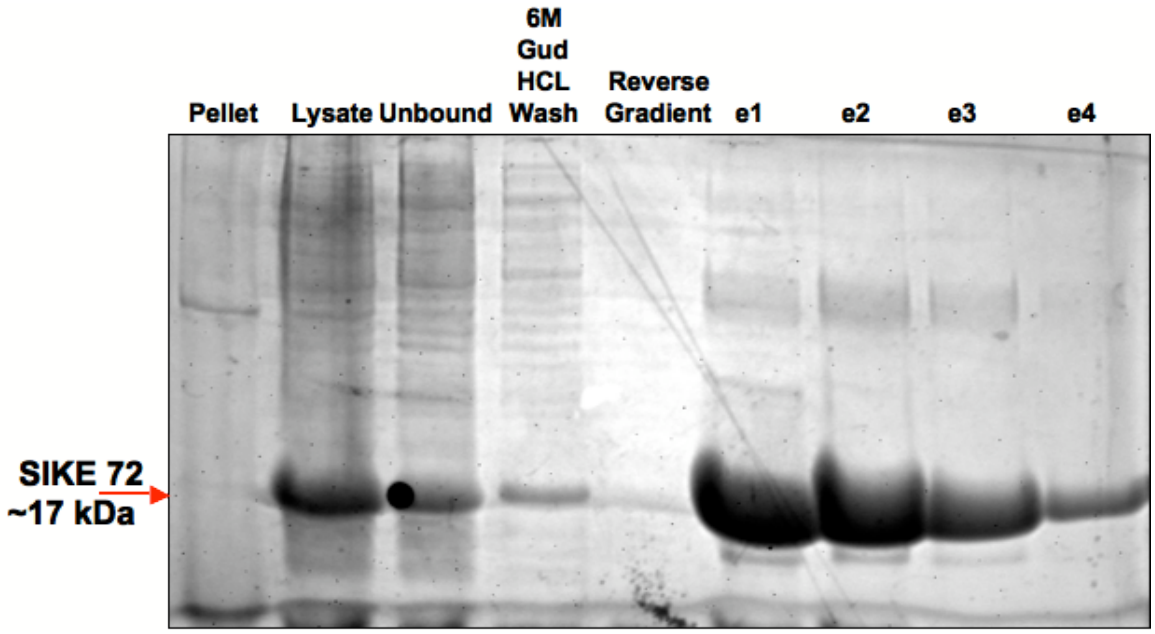


**Figure 9. Refolding of SIKE 72-207 From BL-21 Codon+ Expression.** Two liters of SIKE 72-207 culture were lysed in 6M Gud-HCL and membrane and organelles were removed by centrifugation and a sample of this pellet was saved (pellet). The lysate from this step was loaded onto a Ni-NTA column and allowed to drain by gravity flow (lysate) and then washed with 100 ml of Gud-HCl buffer (Unbound). Column was then subjected to a reverse gradient to remove all guanidine (Reverse Gradient). Protein was eluted using 5 volumes of 5ml of elution buffer (0.5M Imidazole). The resulting elutions are numbered e1 to e4.

**Figure 10. Refolding of NAP 1-270, NAP 1-255 From BL-21 Codon+ Expression**

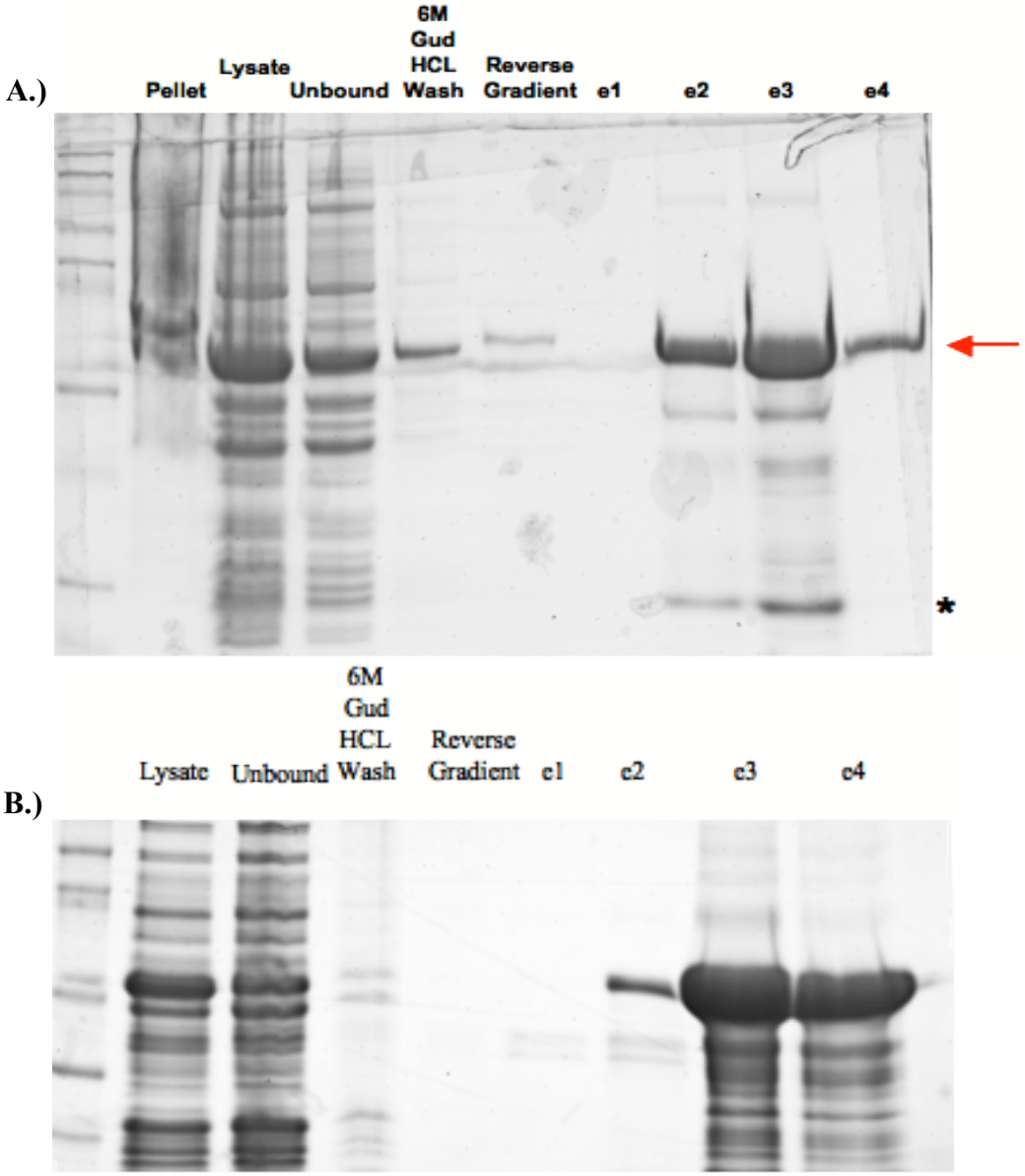


**Figure 10. Refolding of NAP 1-270, NAP 1-255 From BL-21 Codon+ Expression. A.)** Two Liters of NAP 1-270 culture was lysed in 6M Gud-HCL and membrane and organelles were removed by centrifugation and a sample of this pellet was saved (pellet). The lysate from this step was loaded onto a Ni-NTA column and allowed to drain by gravity flow (lysate) and then washed with 100ml of Gu-HCl buffer (Unbound). Column

was then subjected to a reverse gradient to remove all guanidine (Reverse Gradient). Protein was eluted using 5 volumes of 5ml of elution buffer (0.5M Imidazole). The resulting elutions are numbered e1 to e4.

* denotes a conserved degradation product. NAP 1-270 is a construct with an isotopic molecular weight of approximately 33.5 kDa.

**B.)** NAP 1-255 was refolded in the same protocol and samples are labeled the same as A. NAP 1-255 had a small degradation portion as well, however it was not pulled through during SEC. NAP 1-255 has an isotopically averaged molecular weight of 29.7 kDa.

When expressed in BL21de3 Codon+ bacteria both constructs separated to the insoluble fraction. These proteins were refolded as described in the methods section. Elution fractions from the IMAC column were prepared for SDS-PAGE analysis and separated on a 10% SDS-PAGE (**Figure 10**). In all preps of NAP 1-270, a significant band at approximately 10 kDa was observed. These recombinant forms of NAP 1-270 and NAP 1-255 were biochemically characterized.

### 3.2 Characterization of Constructs

#### 3.2.1 Size Exclusion Chromatography (SEC)

Purified, refolded target proteins were subjected to size exclusion chromatography (SEC) separation, which provided information about the oligomeric structure and molecular size of the constructs. In an SEC experiment, macromolecules in solution tumble as spherical species and are separated based upon their ability to interact with resins containing different size pores. Species too large to interact with the resin elute first whereas species that interact with resin/pore elute later allowing for a size distribution of species to be determined. Molecular weights of species can be derived by comparison to a standard curve of globular proteins with well-defined molecular weights. In the set of proteins under study here, the coiled coil domains found in each construct forms a non-globular, helical rod. When tumbling in solution, these coiled coil domains give an apparent hydrodynamic radius that correlates with a much larger species than the actual construct. While SEC can give information on purity and stability of target proteins, the

actual size determination can only be loosely applied. For example, in previous research, SEC of the NAP 1-200 coiled-coil domain produced peaks that corresponded to a hexamer and a 12-mer, but when analyzed by another technique were found to be monomer and dimer species (R. J. Call personal communication). The SEC chromatographs for SIKE FL (26kDa) and SIKE 72 (17.5 kDa) are shown in **Figure 11**. SIKE 72 formed a stable, single species, and was used for all subsequent analysis. Size correlation showed the non-aggregate peak corresponded to 66 kDa (a tetramer). Separation of peak fractions by SDS-PAGE shows that the single peak contained a single band corresponding to SIKE 72 (**Figure 11b**). SIKE 72 fractions were pooled and used for further analysis. Approximately 2-3 weeks after pooling, SIKE 72 would aggregate and precipitate out of solution.

NAP 1-270 (35 kDa) and NAP 1-255 (32 kDa) SEC show that each construct contained non-aggregate but multiple species (**Figure 12, Figure 13**). A sloping shoulder on the lagging edge of the major peak in both constructs suggests multiple species are present. SDS-PAGE analysis of the fractions from the NAP 1-270 SEC showed that the lagging edge had a contaminant protein at ~10 kDa (**Figure 12b**). This band was shown by western blot to incorporate a 6X His-tag (**Figure 12b**), indicating that this protein is a C-terminal truncation of the full NAP 1-270 construct and was likely responsible for the lagging shoulder peak in the SEC chromatograph. Interestingly, the smaller, clipped fragment of NAP1-270 that retains portions of the N-terminal coiled-coil domain

**Figure 11. SEC of SIKE 72-207.**

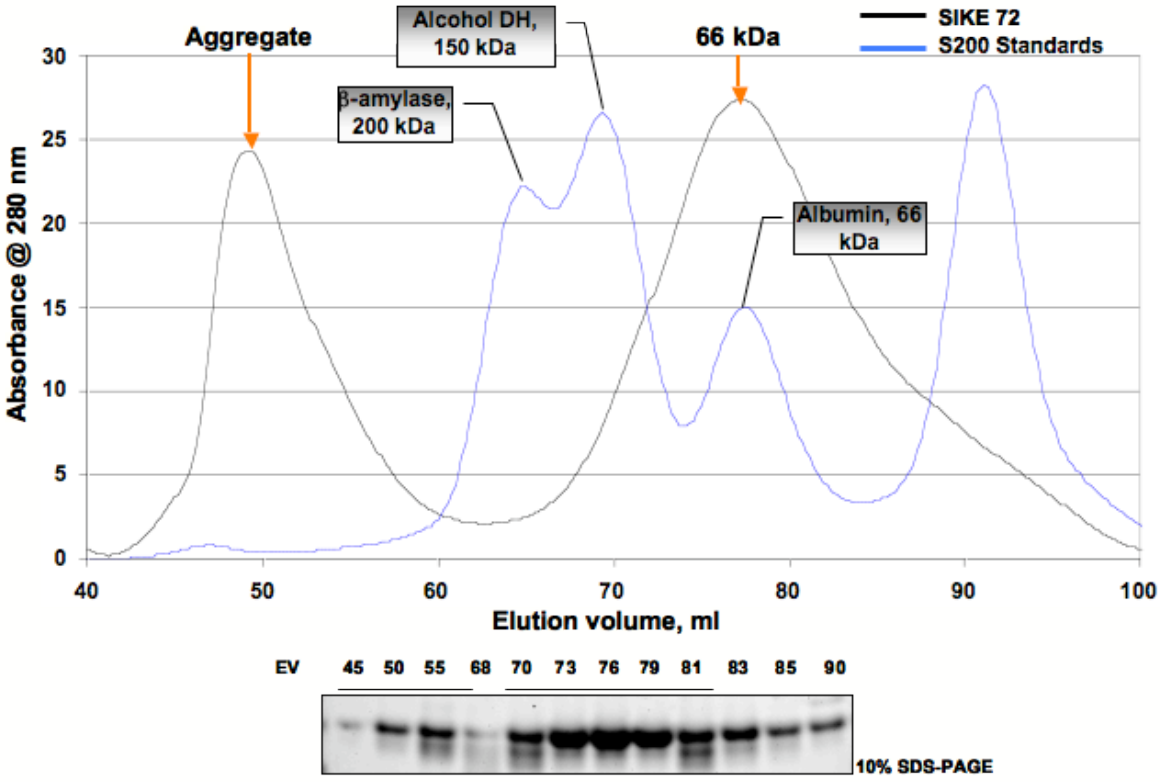


**Figure 11. Size Exclusion Chromatography of SIKE 72-207.** Elutions from the refold were loaded in 5ml quantities onto a s200 column and run in Buffer 4. All 5 fractions had the same profile, with various differences between concentration of aggregate and the single species. Size correlation of the main species fcorrelates to approximately 66 kDa based on globular standards. The resulting SDS-PAGE analysis of the elution fractions is represented in B, and you can see that the protein is pure. This indicates that the differences in elution volume are based on self-associations not contaminant products.

**Figure 12. SEC of NAP 1-270 and SDS-PAGE Analysis of Elution Fractions**

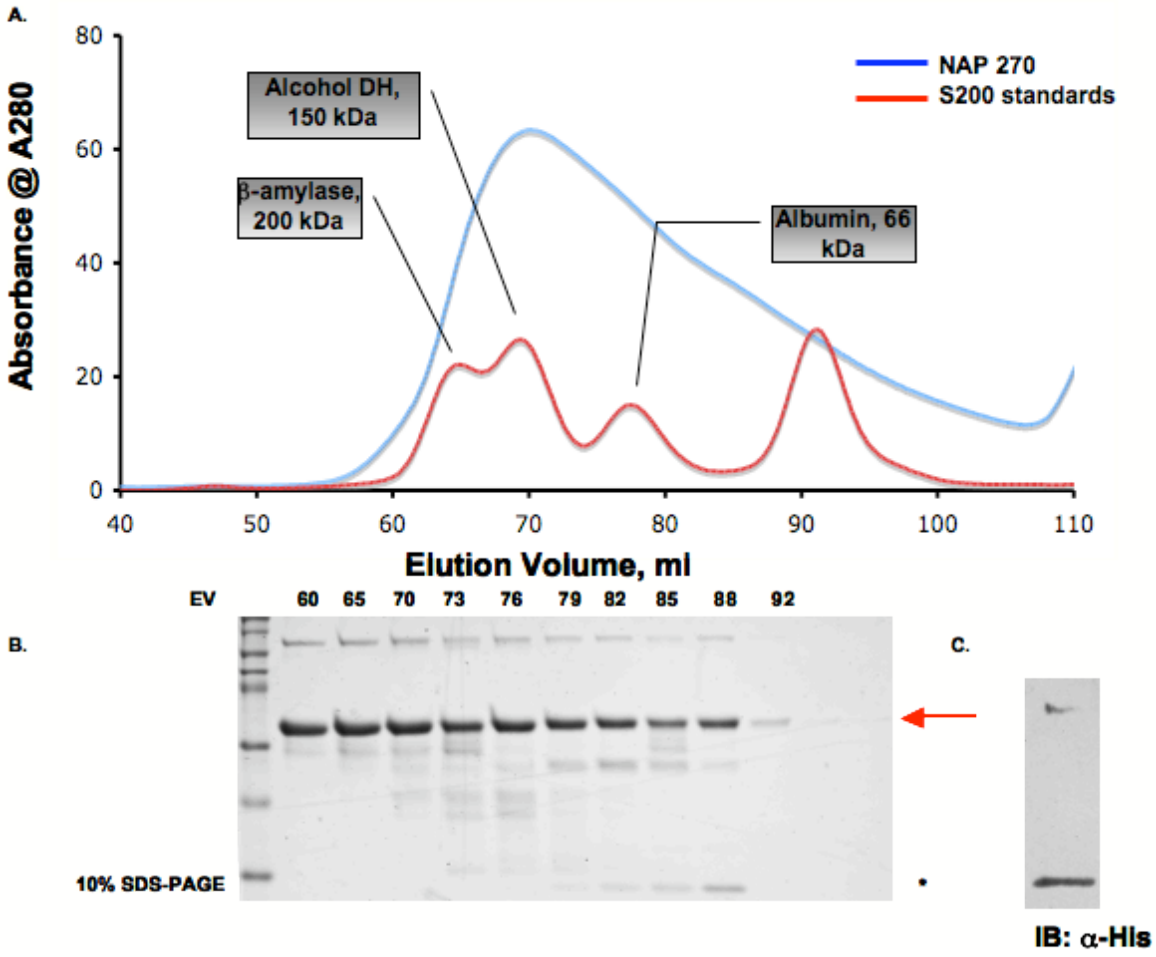


**Figure 12. SEC of NAP 1-270 and SDS-PAGE Analysis of Elution Fractions A.** Elutions from the refold were loaded in 5ml quantities onto a Superdex™ 200 16/60 prep grade column (GE Healthcare) and run in Buffer 4. All 5 fractions had the same profile, with various differences between concentrations of the main peak. As you can see, there is an extreme shoulder on the lagging edge of what is the main species. This indicates that there is more than species present. **B.** Resulting analysis of every other elution fraction confirms the SEC characterization. From the leading edge to the back end of the peak, an increase in smaller species at ~25kDa and ~10kDa (denoted with asterisks) is seen. **C.** Western blot of protein from fraction 88 with a 6X His antibody. This shows that the lower band incorporates a His-tag, indicating that this is a C-

terminal truncation of the full construct. With this knowledge in hand, only the leading 8 fractions were pooled for further study.

**Figure 13. SEC of NAP 1-255 and SDS-PAGE Analysis**

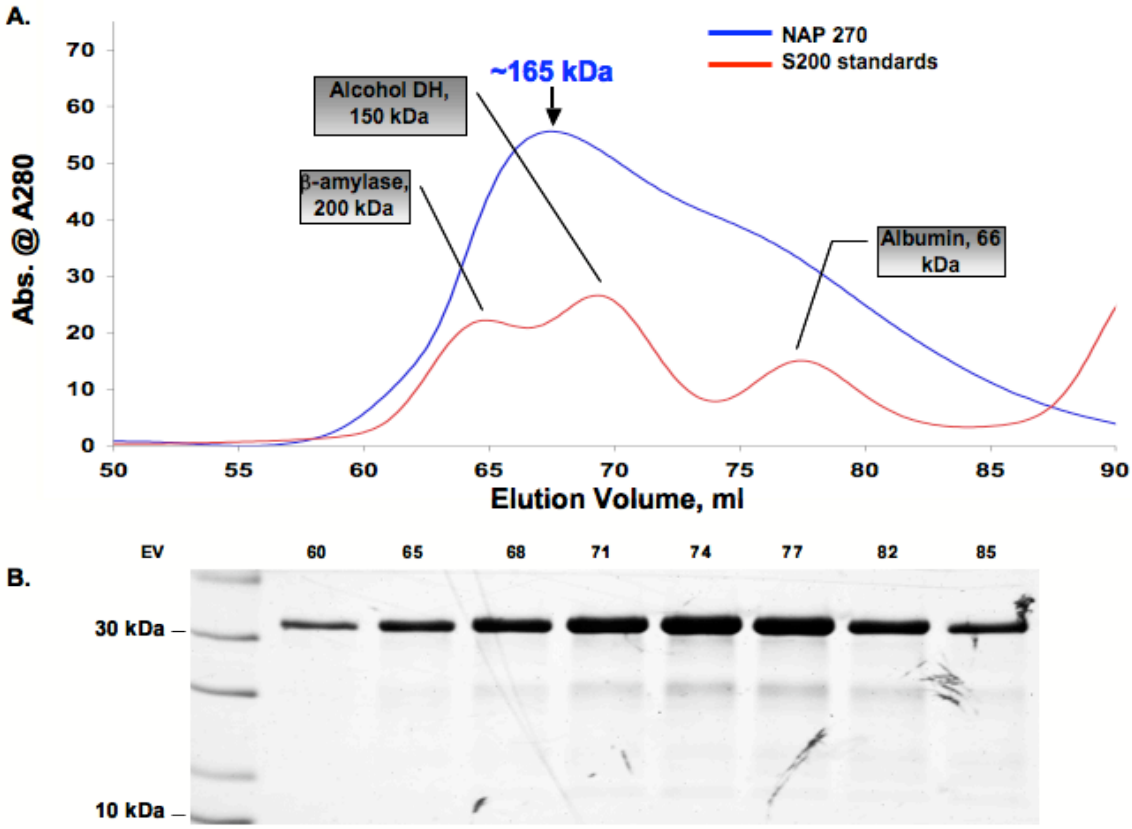


**Figure 13. SEC of NAP 1-255 and SDS-PAGE Analysis of Elution Fractions A.** Elutions from the refold were loaded in 5ml quantities onto a Superdex™ 200 16/60 prep grade column (GE Healthcare) and run in Buffer 4. All 5 fractions had the same profile, with various differences between concentrations of the main peak. An extreme shoulder on the lagging edge of what is the main species is observed. This indicates that there is more than species present. **B**. Resulting analysis of every other elution fraction confirms the SEC characterization. There were no smaller species of the NAP255.

retains a His-tag, indicating is it a C-terminal trunction of our full length construct. Fractions from NAP 1-255 showed a clean sample, with a single band at ~32 kDa (**Figure 13)**. Based on the domain structure of NAP 1-255, the elongated peak may represent protein in a self-associated species, while the lagging edge represents protein in monomer state. For further analysis, the leading edges of SEC peaks (corresponding to the first 8 fractions of the peak and never extending past the mid-line of the first major peak) for both constructs were pooled and concentrated.

TBK-1 (83 kDa) purification was carried out as described in the Methods section. The SEC chromatograph of the purified kinase and SDS-PAGE analysis of peak fractions is shown in **Figure 14**. The single species correlates to a molecular weight of ~ 130 kDa (1.5-mer). This could correspond to either a monomer-dimer equilibrium or an non-globular monomer.

### 3.2.2 Complexing Interactions

One of the driving points of my research was to establish the criterion that is necessary for the formation of a complex between NAP constructs and full length TBK-1. To further pursue the structural importance, it would be necessary to confirm *in vitro* if the kinase binding domain (KBD) of NAP1, previously identified by immunoprecipitation assays, directly mediated this interaction **[30].** This would allow for further study utilizing sequence mutations to identify the critical interaction points. Previous research had

**Figure 14. SEC of TBK-1 and SDS-PAGE Analysis**

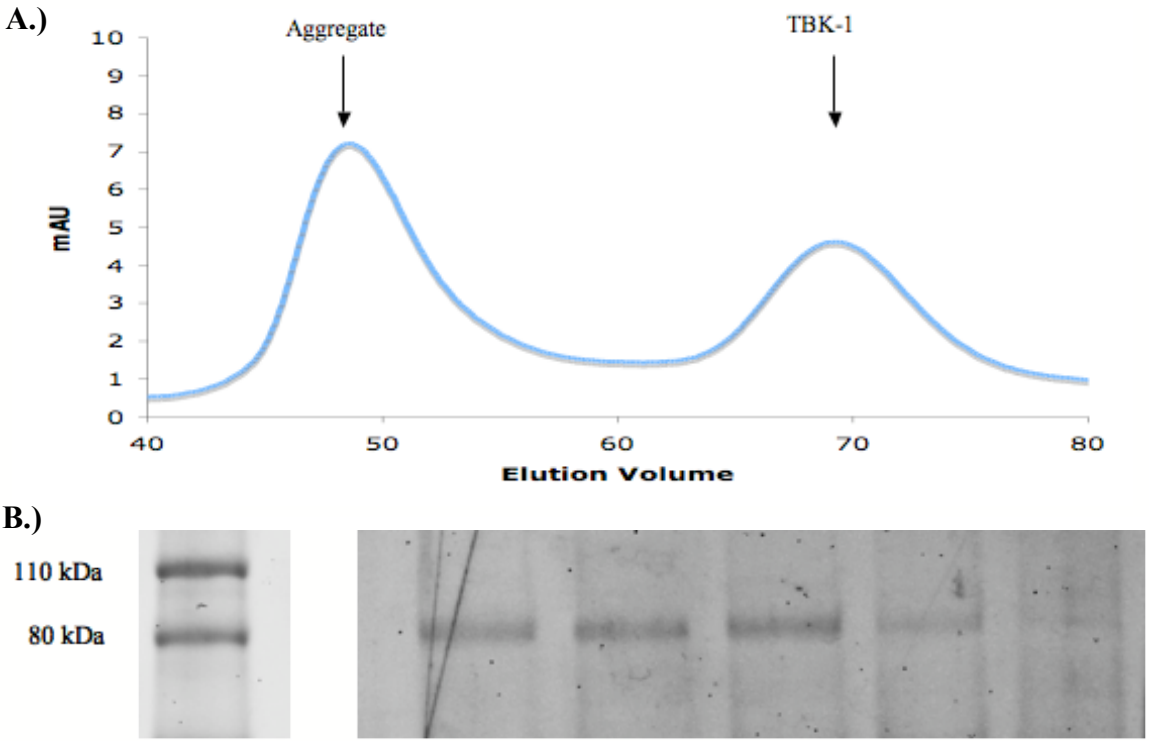


**Figure 14. SEC of TBK-1 and SDS-PAGE Analysis. A.** Bacmid derived TBK-1 elution fractions were separated in Buffer 4 on a Superdex™ 200 16/60 prep grade column (GE Healthcare). All 5 fractions had the same profile, with various differences between concentrations of the two peaks. **B**. Resulting analysis of every other elution fraction from the second elution peak confirms the SEC characterization. TBK-1 was pure and stable.

established that sequences between residues 198-270 were necessary to immunoprecipitate TBK-1 *in vivo* and a potential kinase binding domain sequence identified at residues 216-255 [**30**]. While the immunoprecipitation data indicates that TBK-1 and NAP1 associate, it fails to show a direct interaction between the two or if post-translational modifications might be required for binding. With regard to the latter, the NAP1-KBD is rich in serines, which could be phosphorylated and alter binding to TBK-1. To initiate this line of experiments, TBK-1 was complexed with both NAP 1-270 and NAP 1-255 and SIKE 72.

NAP 1-270 was complexed with recombinant TBK-1 that had been previously purified and stored at –80°C. Each protein was incubated both alone and in protein complex in gel filtration buffer (Buffer 4) in a 1:1 molar ratio overnight at 4°C. These incubation reactions were separated consecutively on Superose™6 Tricorn™ column in buffer 4. Chromatographs for each run are shown in **Figure 15**. Comparison of TBK1 SEC separation during purification versus the TBK1 used in this complexing reaction show additional peaks in the TBK1 sample that had been frozen. These results indicate that TBK1 should be used immediately after purification or conditions for freezing need to be optimized to retain stable TBK1 structure. Also, based upon the clipping observed during purification of NAP 270 and the additional species present in the SEC separation due to this fragment, the NAP 1-255 construct would be better suited for protein interaction studies with TBK1. No SDS-PAGE analysis was completed on peak fractions due apparent degradation of TBK1 component.

**Figure 15. SEC of Complex of NAP 270 with TBK1.**

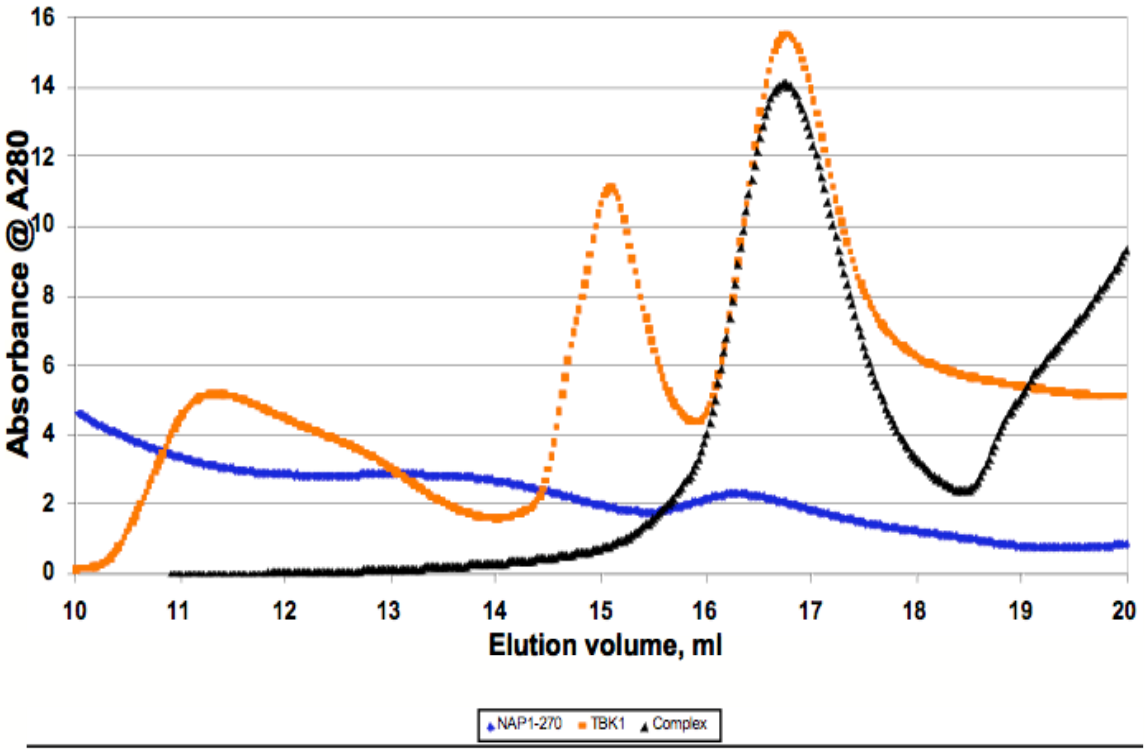


**Figure 15. SEC of Complex of NAP 270 with TBK1.** Pooled NAP 270 from SEC of the refold was allowed to complex with purified TBK-1 that had been frozen down by Jason Call. Samples were set up as per methods, and loaded onto a Superose™ 6 Tricorn™ SEC Column. The resulting chromatograms are depicted. TBK-1 ran in an altered state, indicating that the freezing protocol and process had adverse effects on stability and state of the protein. Based on this, no SDS-PAGE analysis was completed due to the fact that TBK-1 might not have retained a native fold so any conclusions that could be drawn would not be ideal.

NAP 255 was purified, pooled, and complexed with freshly prepared TBK-1. Both proteins were concentrated (NAP255: 0.155 mg/ml TBK1: 0.113 mg/ml) and mixed in a 1:1 molar ratio or incubated alone at the same concentration. Samples were incubated overnight at 4°C and separated on the Superose™ 6 Tricorn™ SEC column. The resulting chromatograms are overlaid in **Figure 16**. Peak fractions from each separation were analyzed by SDS-PAGE, Figure **16 b-d**. Neither the chromatograms nor SDS-PAGE analysis conclusively state that a TBK1:NAP 1-255 complex has formed. While no peaks shift location, also no split peak indicating two distinct species is seen. Complicating the interpretation, TBK-1 and NAP 1-255 elute at almost the same volume. Based on band intensity from the SDS-PAGE, NAP 255 is more concentrated towards the leading edge of the peak and TBK-1 is more concentrated towards the middle fractions of the peak. This indicates that these particular proteins may not interact but co-elute. While TBK-1 runs as large monomer, addition of a single NAP monomer would only shift peak location by approximately 0.25ml based upon this column's separation parameters.

In addition to complex formation assessed by SEC, a simple co-precipitation experiment was completed. Recombinant TBK-1 from insect cells contained an N-terminal FLAG®-tag. The NAP 1-255 construct contained an N-terminal 6X His-tag. For this in vitro co-precipitation experiment, two proteins containing different tags were incubated together. Resin capable of binding one of the two proteins was added to the incubation and allowed to bind its target protein. Resin was pelleted to remove from solution the target protein directly associated with the resin but also any protein capable

**Figure 16. Complex of NAP 255 with TBK1**

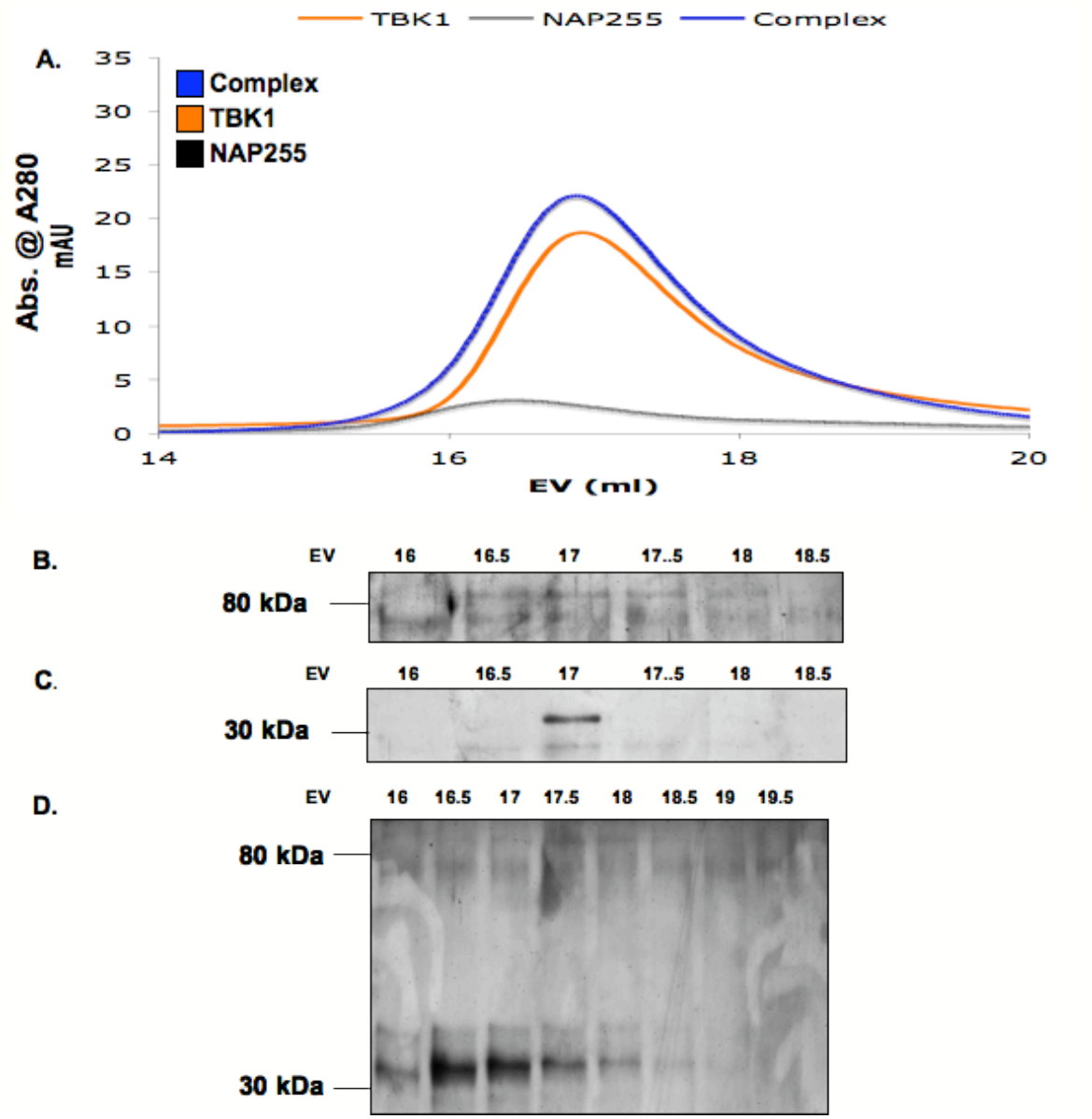


**Figure 16. Complex of NAP 255 with TBK1 A**. SEC Chromatograms of NAP 255 alone, TBK-1 alone and incubated NAP 255 – TBK-1 complex. Samples were run in a total volume of 500ul in a 1:1 molar ratio on the Superose™6 Tricorn™Agarose column. This column was chosen for the potential increase in size of a complex formation. No discernible shift in peak location from complex is observed, however this could be due to the ratio of TBK-1 to NAP with regards to homologous interactions. **B.** SDS-PAGE analysis of TBK-1

alone, and the bands are located at approximately 83 kDa. **C.** SDS-PAGE analysis of the six elution fractions from NAP 255 correlating to the peak and lagging fractions. Majority of sample was located in the main peak, as you can see from the band at 31 kDa in the third fraction. **D.** SDS-PAGE analysis of each fraction under the peak for the complexing interaction. A higher concentration of NAP 255 on the leading edge, and a gradual increase and decrease of TBK-1 as you progress across the peak Is observed. Based on the location of the concentrations of the two constructs and the fact that there is no mutual overlap of concentrations, it is possible that complexing did not occur.

of binding the target protein. Resin was washed to remove loosely bound or non-specifically bound proteins. Bound proteins were released by addition of SDS and boiling. Samples, including starting material, were analyzed by SDS-PAGE. Control included individual proteins incubated with resin and resin alone. The protocol was carried out as described in methods. Initial experiments using FLAG® resin to precipitate TBK1 failed to directly pull down NAP 1-255. This result was found to be due to NAP 1-255 degradation by the time of its use. A new prep of NAP 1-255 was completed; however by this point TBK1 had degraded to a sufficient point that, again, the experiment was not conclusive. Preps for both TBK1 and NAP 1-255 were re-done with an eye towards having freshly purified protein of each construct at the same time. Inclusion of the starting material lanes also allowed direct analysis of the exact concentration used for the co-precipitation. Incidentally, a fresh preparation of SIKE 72 was also completed at this time. Proteins were complexed and co-precipitated as per methods. The SDS-PAGE and subsequent western blot utilizing α-Flag and α-His antibodies is shown in **Figure 17.** TBK-1 pulled down both the SIKE 72 and the NAP 255 construct, however upon addition of both, TBK-1 seems to have a higher affinity towards NAP255, indicating that without any post-translational modifications NAP might have a higher affinity for TBK-1.

### 3.2.3 Circular Dichroism and Thermal Melt

When a refolding protocol is used to obtain recombinant material, one must confirm that a native, folded state has been reached. For proteins having enzymatic

**Figure 17. Co-precipitation of NAP 255 and SIKE 72 with TBK1.**

**A.**

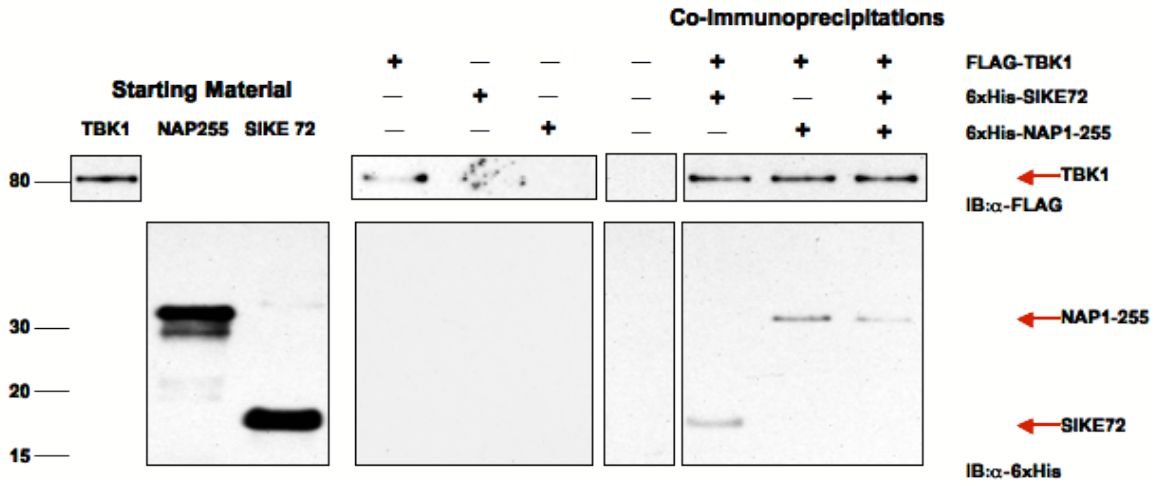


**Figure 17. Co-Precipitation of NAP 255 and SIKE 72 with TBK1.** A. 20 μg of 6X-His-tag NAP255 or 6X-His-tag SIKE72 alone or in combination were allowed to complex for 1 hour on ice with 10 μg Flag®-tag TBK-1 in buffer 4. Samples were then diluted to 1 ml in buffer 4. Controls of each protein alone, along with buffer were incubated with anti-Flag® M2 affinity agarose gel (20 μl) overnight on a circular rotator. After washing and boiling, samples were separated by SDS-PAGE and transferred to nitrocellulose membrane for immunoblotting with α-Flag or a α-6X-His antibody. Resulting western blots are depicted. A.) Starting material was homogenous for all samples with the exception of a small cleavage of NAP255. TBK-1 was pulled down in all reactions it was added too, indicating that the affinity tag was intact. α-Flag resin had no affinity for either NAP255 or SIKE72 alone. Subsequent addition of SIKE 72 and NAP255 constructs with TBK-1 allowed them to co-precipitate. Upon addition of all three proteins, NAP255 co-precipitated with

TBK-1 however SIKE 72 was now absent. While densitometry was not completed, the NAP255 that was pulled down in the presence of TBK-1 and SIKE 72 is less concentrated.

activity, a simple assay confirms a native fold. In the absence of a functional assay, presence of stable secondary structure can be used as an indicator of a folded protein. Neither SIKE nor NAP1 constructs can be functionally assayed so circular di-chroism (CD) spectra were collected on these constructs to confirm secondary structure content and stability. CD

spectra and thermal melt of the constructs NAP 270 (**Figure 18)** and NAP 255 (**Figure 19**) show that both have alpha-helical character as expected for their coiled coil domains. However, their thermal melt profiles show significant differences in their secondary structure stability. NAP 270 has very little stepwise loss of helical content occurring as temperature increases. A straight line is included for comparison. This indicates while alpha-helical character in the coiled coil domain is intact the overall tertiary interactions are weak or absent. Looking at the NAP 255 thermal melt, stepwise loss of alpha helical content to unfolded state can be followed indicating a potential non-monomer association and a stable tertiary structure. The thermal melt data suggests that the NAP 255 construct contains tertiary/quaternary structure.

### 3.2.4 Analytical Ultracentrifugation

Final determination of the oligomeric state of the constructs was completed using analytical ultracentrifugation (AUC) sedimentation velocity (SV) experiments. Numerous complications were overcome to collect data. First and foremost, the constructs had limited solubility. Buffers ideal for AUC, without stabilizing agents such as high salt, glycerol or a reducing agent (DTT or BME), greatly diminished target protein solubility. Use of glycerol

**Figure 18. Circular Dichroism and Thermal Melt of NAP 270.**

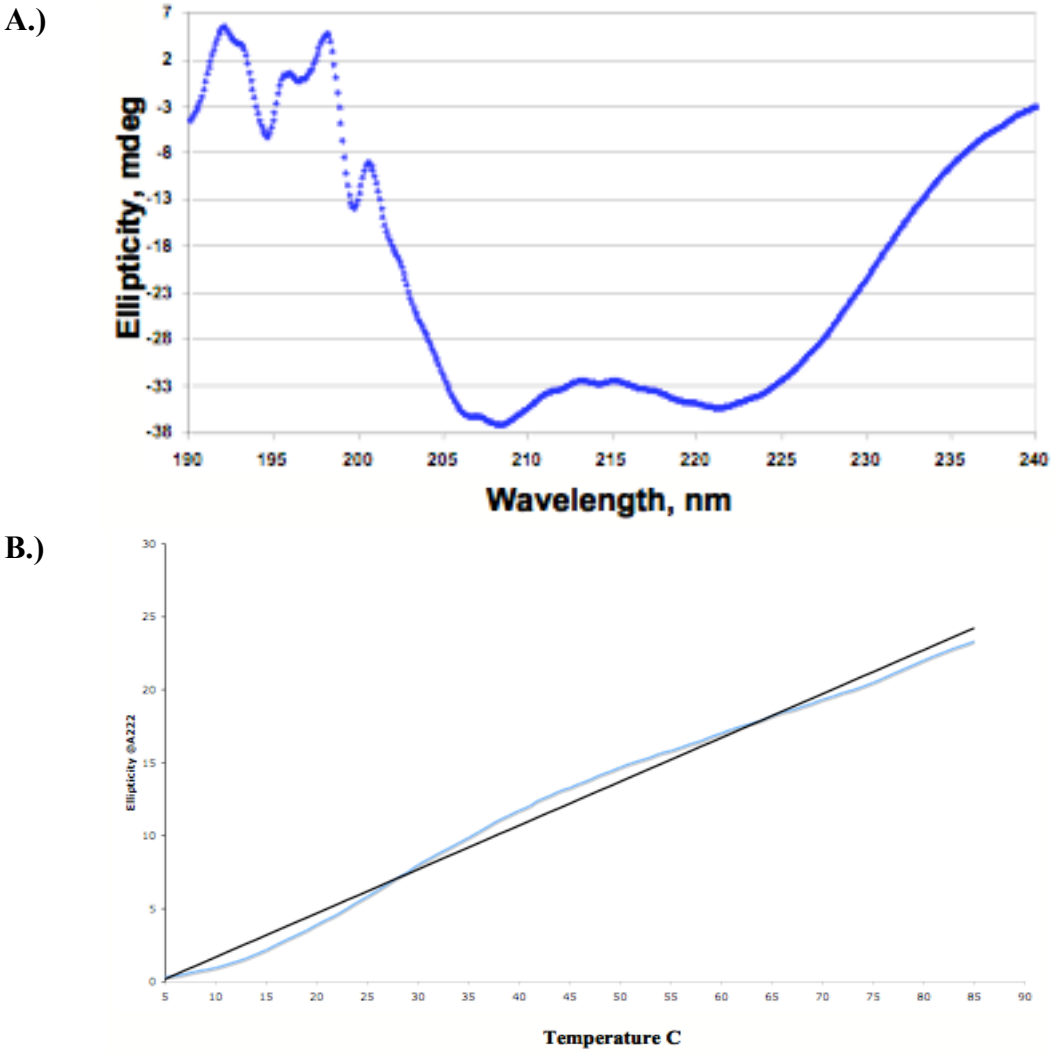


**Figure 18. Circular Dichroism and Thermal Melt of NAP 270**. Samples of NAP270 from SEC experiments were dialyzed into 0.05 M Phosphate pH8 and 0.05 M NaCl. Dialysis buffer was kept as a blank. Samples were scanned 5 times, and the results were averaged by Jasco CD Software. Sample was then subjected to a thermal melt from 4 °C to 85 °C measuring ellipticity at $A_{222}$. CD spectra indicate an alpha-helical structure, while the thermal melt shows negligible stepwise function for unfolding.

**Figure 19. Circular Dichroism and Thermal Melt of NAP 255.**

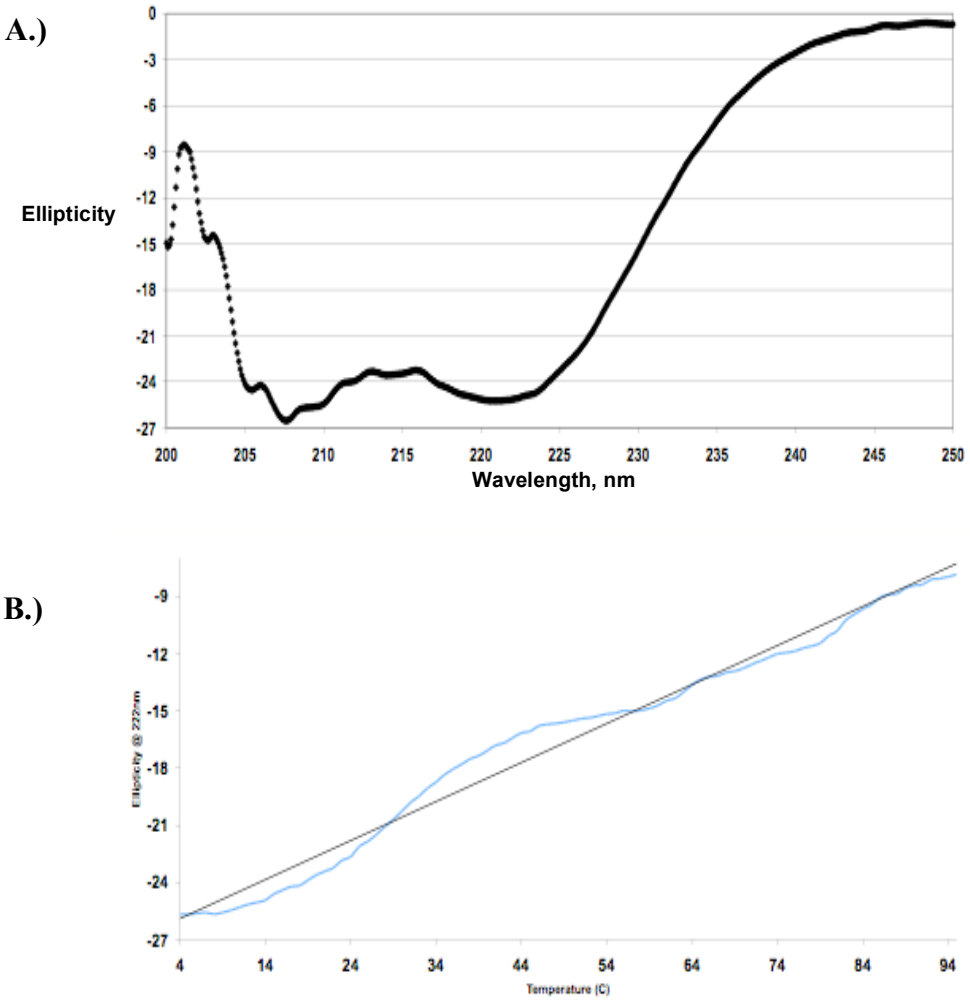


**Figure 19. Circular Dichroism and Thermal Melt of NAP 255.** Samples of NAP 255 from SEC experiments were dialyzed into 0.05 M Phosphate pH8 and 0.05 M NaCl. Dialysis buffer was kept as a blank. Samples were scanned 5 times, and the results were averaged by Jasco CD Software. Sample was then subjected to a thermal melt from 4°C to 95°C measuring ellipticity at $A_{222}$. CD spectra indicate an alpha-helical structure, while the thermal melt shows negligible stepwise function for unfolding.

in any quantity in the buffer also complicates data analysis as glycerol can participate in the hydration sphere around the target protein and also sediment alone, both properties affect determination of target protein sedimentation coefficients. In addition, glycerol directly affects interference data, due to its viscosity. Both DTT and BME absorb in the spectrum that is scanned (usually $A_{280nm}$), and were therefore eliminated from buffers. With these limitations the buffer used for initial AUC data collection was 20mM HEPES, pH 7.5, 300mM NaCl. Samples of pooled and purified construct were concentrated to an $A_{280nm}$ of approximately 1.0. Samples were dialyzed overnight in to AUC buffer to provide a buffer blank for SV experiments. Overnight dialysis of the construct into the original AUC buffer resulted in large amounts of aggregate and significantly reduced protein concentration in solution. In addition, this aggregation left a buffer matching problem, as salts would aggregate with protein and would be removed when aggregate was spun down. The fringe residuals were significantly different (>0.2) between buffer alone and buffer with protein that could not be attributed to protein. Even with the best-fit data correlation of the program, the residuals were still consistently large down the length of the cell. This data could not be used to conclusively determine oligomeric state.

In addition to sample difficulties, equipment failures also contributed to unusable data runs. On numerous runs, the interference and absorbance data would be unusable due to either malfunction of the collecting laser or buffer matching problems. Temperature fluctuations were also noted. Numerous data collections were scrapped due to the fact that the radiometer would record a temperature outside of the acceptable stable range of +/- 1

°C. Due to these issues, the optics system in the centrifuge was finally replaced, and the temperature stability issue addressed.

Based on the fact that NAP 1-270 was more stable to 4°C, data collection for NAP 1-270 using the original buffer were completed at 4°C. However, due to a data collection error, the computer stopped collecting data after 31 scans. The collection error stemmed from the inability of data transfer between centrifuge and computer to occur on a fast enough timescale to allow the machine to reset for the next scan. To overcome this error, time per scan of cells was increased to 6 minutes. However, interference scans on 2 of the 3 cells are still consistently unusable.

Instead of pursuing NAP 1-270 that included a fragment, the NAP 255 construct was used for further AUC analysis. To increase stability of constructs, glycerol but less salt was added to the AUC buffer. To account for the hydration and sedimentation effect of glycerol, parameters in the data analysis software were established by collaborator, Dr. John Burgner. The final buffer composition was 20mM HEPES, pH 7.5, 150mM NaCl and 5% glycerol. Two runs of the exact same protein sample were collected at $A_{280nm}$ of 0.4 and 0.2. The data plot and fringe residuals are shown in **Figure 20**. The difference between runs 1 and 2 was that in run 1 samples were allowed to equilibrate overnight at 4°C in the cold room and then quickly transferred to the centrifuge versus in run 2 samples were equilibrated at 4°C in the centrifuge. The second run was used to account for any convection effects due to change in temperature between cold room, loading of cells and placement in centrifuge in run 1.

**Figure 20. Analytical Ultracentrifugation Best-Fit Analysis of NAP255.**

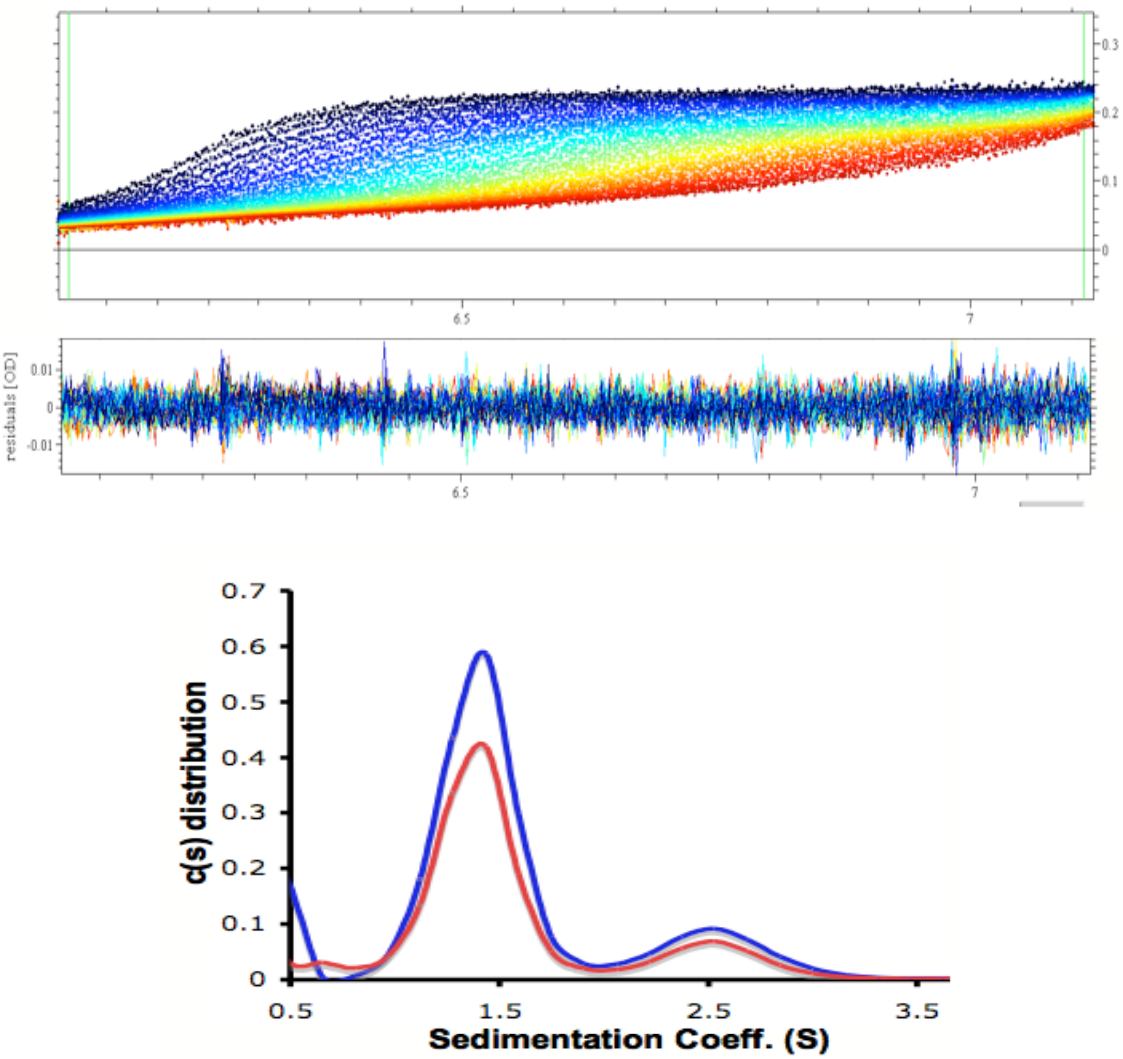


**Figure 20. Analytical Ultracentrifugation Best-Fit Analysis of NAP255**. Best-fit correlation of data from NAP255 using SEDFIT. Top panel depicts the Data plot, middle panel depicts residuals and the bottom panel is the C(s) distribution of the two concentrations of NAP 255 tested. Residuals are small, indicating a good fit of the proposed model to the experimental data. The resulting correlated molecular weights and relevant parameters used are listed in Table 3. The blue line is 18 μM and the red line is 9 μM.

Best-fit analysis using SEDFIT were applied to the data plots from **Figure 20** and gave residuals that were small (<0.01). All scans were completed giving reliable results to base analysis on for both runs. **Table 3** reports parameters derived from the data. The continuous sedimentation distribution plot shows that the major species' sedimentation coefficient (S) correlated to a molecular weight of 34.2 kDa (Expected monomer weight of 32.2 kDa). Interestingly, the predicted S value of a dimeric NAP 1-255 was exceeded by both samples for the second species. If the coiled-coil domains interact in anti-parallel configuration, the KBD of each would extend past the self-associated coiled coil domain region. This S value could also be attributed to the fact that SEDFIT uses the best frictional coefficient to match the data, and the frictional coefficient for the dimer species, if it interacts anti-parallel, would be larger. The failure to account for the difference in the frictional ratio of the monomeric versus dimeric species could skew the predicted S value larger, which in turn could give the correlated molecular weight of approximately a 2.5-mer. Based on these analyses, no concentration dependence for the monomer-dimer equilibrium, measured at 18.7 μM and 7.9 μM, was observed. Collection of data for SIKE 72 using the latest buffer was also collected. The data plot, residuals and C(s) for SIKE 72 are represented in **Figure 21.** Three distinct species are identifiable, corresponding to a monomer, dimer and tetramer. Their C(s) distribution peaks have their MW listed in **Table 3**, along with relevant parameters from the best-fit analysis.

Figure 21. Analytical Ultracentrifugation Best-fit Analysis of SIKE 72

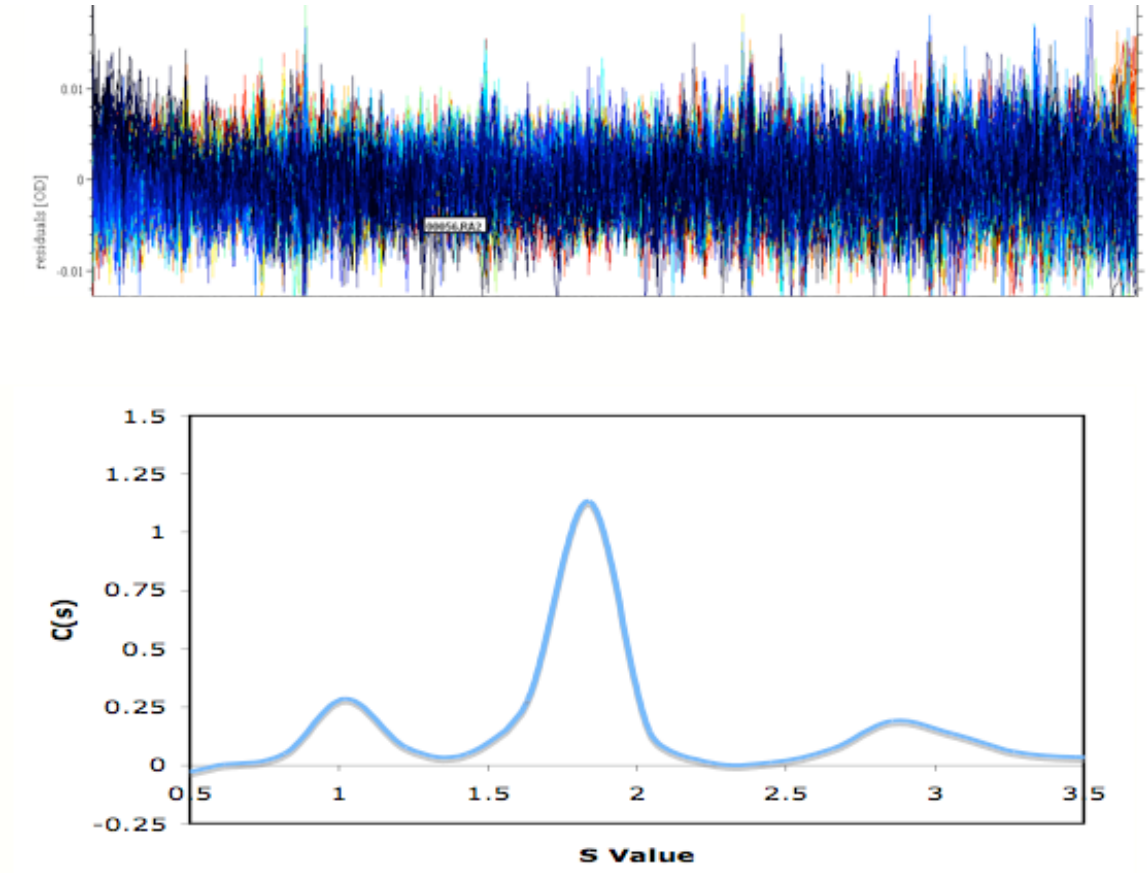


**Figure 21.Analytical Ultracentrifugation Best Fit Analysis of SIKE 72.** Best-fit correlation of data from SIKE 72 using SEDFIT. Data plot was omitted. Top panel depicts residuals and the bottom panel is the C(s) distribution of SIKE 72 tested which was 16.5 μM. As you can see, residuals are small, indicating a good fit of the proposed model to the experimental data. The resulting correlated molecular weights and relevant parameters used are listed in Table 3.

**Table 3. Relevant Values from Best-Fit analysis of NAP 255 and SIKE 72.**

| Sample | $f/f_0$ | S-Value | Mass (kDa) | RMSD |
|---|---|---|---|---|
| **NAP 255** | | | | |
| **Overall** | **1.34** | | | **0.0048** |
| **Peak 1** | | **1.42** | **34.2** | |
| **Peak 2** | | **2.65** | **82.1** | |
| **SIKE 72** | | | | |
| **Overall** | **1.09** | | | **0.0053** |
| **Peak 1** | | **1.24** | **18.5** | |
| **Peak 2** | | **1.79** | **33.2** | |
| **Peak 3** | | **2.98** | **68.9** | |

### 3.2.5 Crystallization

Crystal screens using purified SIKE 72-207 at 6.98 mg/ml were attempted. A factorial screen, Qiagen Classics Suite 96-well screen, was prepared and incubated at 18°C. Initial screens were visualized approximately 2 weeks after preparation. Wells were scored 1-10 according to a scale developed by Hampton Research, 1 being clear with the appearance of precipitate scoring a 3, crystalline material a 5, needle-like crystals a 7 and individual crystals a 10. In the initial 96 conditions, approximately 30 conditions had a score greater than 5, with none exceeding 7. Review of the conditions showed that SIKE 72 had a proclivity for polyethylene glycol (PEGs) conditions. A second 96-well screen was prepared using the Qiagen PEGs Suite, and a protein concentration of 4.98 mg/ml. Review after 2 weeks showed the a similar range in scoring. However, 4 months post-loading review showed a crystal formation in the buffer 0.2M KF and 20% PEG3350. Subsequent loading and x-Ray diffraction of this crystal showed both high resolution diffraction consistent with salt crystals and low resolution powder diffraction consistent with protein. Additional experiments need to be designed to determine whether or not 0.2M KF and 20% PEG 3350 or some minor alteration will crystallize SIKE 72.

## 3.3. Mammalian Cell Co-Immunoprecipitation

HEK293 Mammalian cells were transfected with pCMV-HA SIKE, harvested and used to immunoprecipitate using Anti-HA agarose as outlined in methods. Two different transfection reagents were used (Fugene®, Lipofectamine®), and samples were run on SDS-

**Figure 22. Immunoprecipitation of HA-SIKE FL**

**A.**

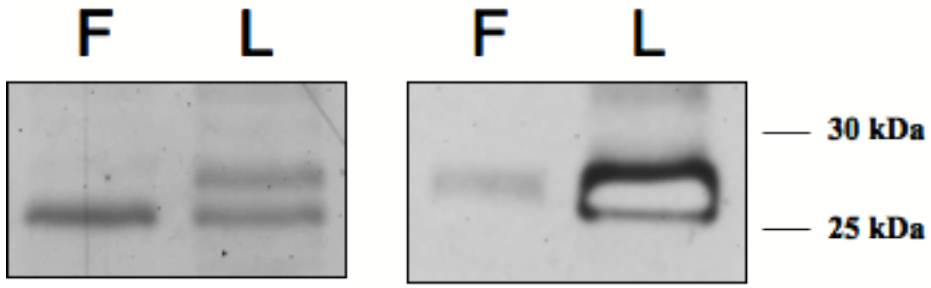


**B.**

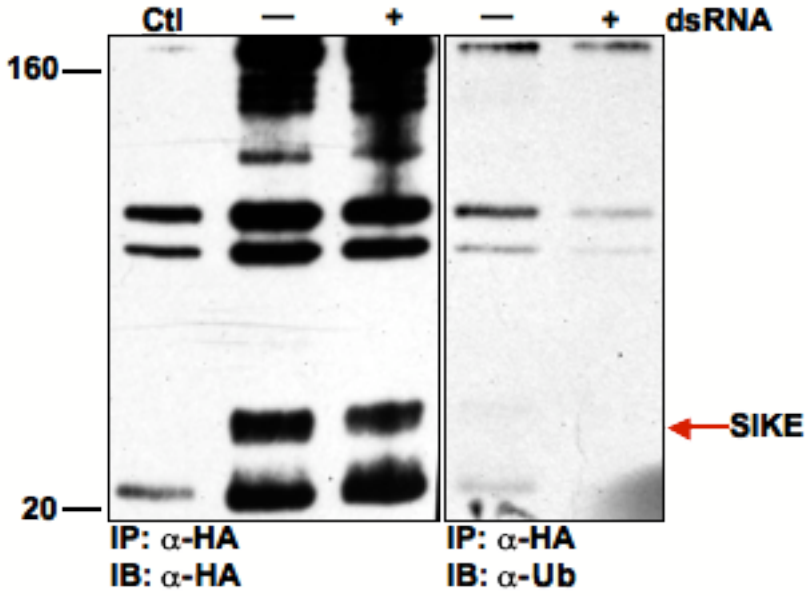


**C.**

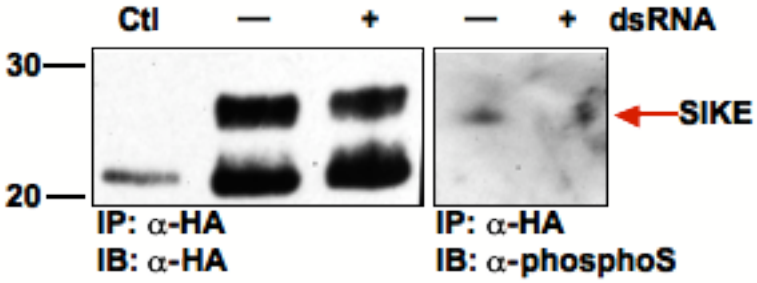

**Figure 22. Immunoprecipitation of HA-SIKE FL. A.** HEK 293 Mammalian cells were transfected with either Fugene® (F) reagent or Lipofectamine® (L) reagent with pCMV-HA-SIKE FL DNA as per methods. Resulting lysates were incubated with 20 μg of α-HA.11 Ab Affinity Agarose overnight. Samples were washed, and loaded onto two SDS-PAGE gels, 20 μl of sample in each. One was visualized by coomassie staining (Left), while another was used for western blot utilizing a Anti-HA antibody (Right). SIKE FL transfection and pull down was successful using Lipofectamine®. **B.** HEK 293 cells were transfected with pCMV-HA-SIKE FL as per Methods. After this point, cells were (un) stimulated with pI:pC for 24 hours. Cell lysates were collected and immunoprecpitated with α-HA resin as per methods. Resulting samples were separated by SDS-PAGE and transferred to nitrocellulose membrane for western blotting. Two separate immunoblots utilizing the HA-IP sample were probed, with α-HA blot represented on the left, and an α-Ub antibody represented on the right. There is no stepwise gain of 10 kDa to the original SIKE sample, indicating it is not ubiquinylated. **C.** HEK 293 cells were transfected with pCMV-HA-SIKE FL per methods and allowed to rest for 24 hours. After this point, cells were (un) stimulated with pI:pC for 24 hours. Cell lysates were collected and immunoprecpitated with α-HA resin as per Methods. Resulting samples were separated by SDS-PAGE and transferred to nitrocellulose membrane for western blotting. Two separate immunoblots utilizing the HA-IP sample were run, with an α-HA blot represented on the left, and a α-phospho-serine on the right. SIKE FL is phosphorylated prior to stimulation with pI:pC, and dephosphorylated post-stimulation.

PAGE and analyzed by western blot. Blots were screened with HA-antibody, and the results from transfection are shown in **Figure 22 A.** Subsequent experiments utilizing pulled down SIKE from mammalian cells were attempted. However, instead of blotting for the HA construct, antibodies for a phospho-serine (SIKE has a predicted phosphorylation site at S74), and for ubiquitin were used to delineate any post-translational modifications. Transfected lysates of 293 cells stimulated with dsRNA for 24 hours and unstimulated were collected and immunoprecipitated as per methods. Subsequent SDS-PAGE and western blot using an anti-ubiquitin (**B**) and an anti-phosphoserine (**C**) antibody are shown in **Figure 22.** SIKE is phosphorylated prior to stimulation, however upon stimulation and activation of the pathway, SIKE is dephosphorylated. The question that remains is whether this phosphorylation is required for binding and inhibition of SIKE to the kinase activity. While SIKE from 293 cells is not ubiquinylated, introduction and blotting of this same construct into immune cells is necessary, as the machinery that might be required for ubiquinylation of SIKE may be absent in 293 cells.

# Chapter 4. Discussion

Protein-protein interaction networks form the backbone of signaling responses. While the field has progressed at a rapid rate in terms of understanding the role of various players to mediate activation/regulation, the interferon pathway of TLR3 present some novel twists. The incorporation of three scaffolds represents a unique element in this pathway [**30**]. While one scaffold has been shown to be both phosphorylated by TBK-1 and K-63 ubiquitinylated, the functional consequences of these modifications on kinase activity are unknown [**27**]. In addition, two alternative scaffolds have been identified, however, with the exception of identifying complexing partners, little insight into their function has been reported [**28,30**]. SIKE interactions and potential complexing partners have been reported [**31**]. However, the mechanism by which SIKE inhibits kinase activity remains unknown. SIKE may act through sequestering the kinases or preventing homo- or hetero-interactions. The role of post-translation modification in SIKE function is completely unexplored. With all these proteins, direct interactions have not been identified, though co-immunoprecipitation experiments imply association between the three functionally different types of proteins involved in the kinase complex of this pathway [**30,31**].

Establishing direct interactions is essential to identifying motifs required for activation or regulation of this system.

Understanding normal activation/regulation of this system may reveal how viral subversion or dysregulation found in disease states evolved. The interferon response partially mediated by the TLR3 pathway can be utilized to selectively target cell populations for death through apoptosis [**36**]. Ebola and Hepatitis C virus, along with a multitude of other infectious agents, have evolved multiple mechanisms to evade this specific signaling response [**3**,**4**]. Inhibiting the interferon pathway, by sequestering the activating ligand, dsRNA, or directly inhibiting signal transduction, has allowed viruses to increase infectivity and replication in a host [**4**]. Therefore, in order to fully understand viral mechanisms of inhibition and to develop a means to prevent or reverse viral subversion, endogenous activation and control of this pathway must be defined.

The potential therapeutic applications of pathway activation have already been documented. Administration of polyinosinic:polycytidylic acid (pI:pC), a synthetic mimic of viral dsRNA, increased expression of type I interferon but caused side effects including shock, renal failure, coagulopathies, and hypersensitivity reactions [**37**]. Intravenous interferon-β, the downstream effector, suffers from a limited half-life [**38**,**39**]. Alternatively, interferon-$\beta$ delivered via replicative-incompetent adenovirus has been shown to illicit a tumor-specific humoral immune response, however down regulation of targeted MCH class expression allowed tumor escape mutants to develop reducing the efficacy of this treatment in clinical trials [**39**]. While preliminary cell-based research has shown that both pI:pC and IFN-$\beta$ can have positive effects with regard to cancer cell apoptosis and

initiation of a selective immune response, implementation of this effect in a clinical setting has met with limited success. With these limitations, one must begin to question what alternative methods need to be approached to activate this pathway. One approach may be selective removal of inhibition. Alternatively, IKK-ε has been show to be hyperactive in breast cancer [**39**] and subsequent knockdown has been shown to induce apoptosis indicating that reinstituting control of this kinase in targeted situations could be an effective avenue of treatment.

While alternative inhibitors can silence portions of the TLR-3 response, SIKE alone stands as the selective inhibitor of TBK-1 and IKK-ε activity [**24,31,33,35**]. The removal of this inhibition allows for phosphorylation of IRF3, required for IFN-$\beta$ transcription. To realize the therapeutic potential of IFN-β, a process to selectively decrease SIKE production or increase SIKE degradation of SIKE or alter its inhibitory properties with respect to activity of TBK-1 and IKK-ε may be beneficial. However, before a system can be altered, its endogenous mechanism to inhibit kinetic activity, and how this inhibition is removed must be defined. My initial studies indicate that a phosphorylation event might be a critical component of this control. With respect to the scaffolds, further study is needed to understand their effect on kinase activity and if scaffold can protect kinase from SIKE inhibition.

The main conclusions from the research presented in this thesis are as follows: First and foremost, SIKE FL and SIKE 72 are mostly insoluble both alone and when co-expressed with either of the kinases. This indicates that SIKE either does not bind directly to TBK1 or IKKε, or does not do so with high affinity, or binding may require post-

translational modification(s), The serine phosphorylation of SIKE observed *in vivo* prior to dsRNA stimulation but absent following dsRNA stimulation may serve as a switch for SIKE:kinase complex. Experiments *in vitro* using SIKE constructs to mimic a phosphorylation event could then be used to elucidate if this phosphorylation event is necessary for complex formation. Future *in vivo* experiments will need to define the phosphorylation site, if, in fact, the phosphorylation site coincides with the predicted serine 74 phosphorylation site [**40**]. Additionally, NAP 270 and NAP 255 are insoluble in bacterial expression. NAP 255 binds to TBK1 *in vitro* as assessed by co-precipitation experiments. Based on this analysis, further studies again utilizing HEK 293 cell transfections of full-length NAP1 and TBK1 have been planned to help delineate the modifications, if any, which might alter the affinity for binding of NAP1 to TBK1.

From AUC experiments, NAP 255 forms mostly a monomer. Our analysis of this data may be biased by the non-ideal buffer conditions required for sample preparation, including the addition of glycerol. Further study by dynamic light scattering that could be coupled to the AUC data may allow a consistent interpretation of the data. As NAP1-200 forms a stable dimer, the transition to a monomer form by the addition of 55 amino acids in NAP1-255 is surprising. By coupling two methods, a better approximation of the oligomeric state may be obtained. As only a single SIKE 72 concentration was analyzed by AUC, more data collected at several concentrations will be necessary to deduce any insight on concentration dependence of oligomeric state. However, initial studies show that SIKE 72 has higher order self-associations predominantly as a dimer. Small amount of tetramer and monomer species are present.

Previous studies showing a complex of approximately 670 kDa that incorporates scaffolds, kinases and SIKE begs the question of stoichiometry within the complex [**31**]. Interestingly, a partial TRAF-3 x-ray structure revealed a trimer subunit arrangement [**41**] would be located upstream of the kinase complex. If working from a trimeric scaffold, three NAP1 dimers could form a platform for six kinase docking events giving a complex of 875 kDa. This higher order complex has been observed for the activation of caspase in the apoptosome [**42**] the inflammasome [**43**] and, more recently, with an innate immune signaling complex involving MyD88, the Myddosome [**44**]. Although precedence exists for large, ordered complexes, we must first better define our potential interaction partners. Experimentation to determine the post-translational modifications of NAP1 are underway, which could lead to significant insight into potential necessity of modifications for complex formation. Competition between scaffold and inhibitor for a single kinase-binding site may determine the inclusion/exclusion from a signaling complex. The most interesting result from this current work was that SIKE was phosphorylated prior to stimulation with pI:pC and dephosphorylated following stimulation. As SIKE is constitutively bound to TBK1 but released upon pathway stimulation, the addition of a phosphate group would suggest this phosphorylation event might be critical to binding. The question remains whether this phosphorylation directly correlate to kinetic inhibition of the kinase. Two key experiments would highlight the role of this post-translational modification: 1) engineer a construct of SIKE that incorporates a phosphomimetic (Glu or Asp) at S74 to assess function and 2) identify the kinase/phosphatase responsible for addition/removal of this post-translation modification. These experiments could lead to either new targets for the

intrinsic control of the pathway or a reveal a novel link between signaling cascades to illicit regulation of the innate immune response.

## Literature Cited

[1-45]


1. Janeway, C.A.T., P. Walport, M. Shlomchik, M.J., *Immuno-Biology; the immune system in health and disease*. 6th ed. 2005, New York: Garland Science. 823.
2. Paul, W.E., *Fundamental Immunology*. 5th Edition ed. 2003, Philadelphia: Lippincott, Williams & Wilkins. 1687.
3. Jin, H., et al., *The VP35 protein of Ebola virus impairs dendritic cell maturation induced by virus and lipopolysaccharide.* J Gen Virol. **91**(Pt 2): p. 352-61.
4. Bowie, A.G. and L. Unterholzner, *Viral evasion and subversion of pattern-recognition receptor signalling.* Nat Rev Immunol, 2008. **8**(12): p. 911-22.
5. Kandyil, R.M. and C.M. Davis, *Shellfish allergy in children.* Pediatr Allergy Immunol, 2009. **20**(5): p. 408-14; quiz 414.
6. Mason, J.M. and K.M. Arndt, *Coiled coil domains: stability, specificity, and biological implications.* Chembiochem, 2004. **5**(2): p. 170-6.
7. Metz-Boutigue, M.H., et al., *Antimicrobial Peptides Present in Mammalian Skin and Gut are Multifunctional Defence Molecules.* Curr Pharm Des, 2009.
8. Lemaitre, B., et al., *The dorsoventral regulatory gene cassette spatzle/Toll/cactus controls the potent antifungal response in Drosophila adults.* Cell, 1996. **86**(6): p. 973-83.
9. Deva, R., et al., *Candida albicans induces selectively transcriptional activation of cyclooxygenase-2 in HeLa cells: pivotal roles of Toll-like receptors, p38 mitogen-activated protein kinase, and NF-kappa B.* J Immunol, 2003. **171**(6): p. 3047-55.
10. Medzhitov, R., P. Preston-Hurlburt, and C.A. Janeway, Jr., *A human homologue of the Drosophila Toll protein signals activation of adaptive immunity.* Nature, 1997. **388**(6640): p. 394-7.
11. Poltorak, A., et al., *Defective LPS signaling in C3H/HeJ and C57BL/10ScCr mice: mutations in Tlr4 gene.* Science, 1998. **282**(5396): p. 2085-8.
12. Visintin, A., et al., *Secreted MD-2 is a large polymeric protein that efficiently confers lipopolysaccharide sensitivity to Toll-like receptor 4.* Proc Natl Acad Sci U S A, 2001. **98**(21): p. 12156-61.
13. Matsumoto, M., et al., *Subcellular localization of Toll-like receptor 3 in human dendritic cells.* J Immunol, 2003. **171**(6): p. 3154-62.
14. Pisegna, S., et al., *p38 MAPK activation controls the TLR3-mediated up-regulation of cytotoxicity and cytokine production in human NK cells.* Blood, 2004. **104**(13): p. 4157-64.

15. Schmidt, K.N., et al., *APC-independent activation of NK cells by the Toll-like receptor 3 agonist double-stranded RNA.* J Immunol, 2004. **172**(1): p. 138-43.
16. Sivori, S., et al., *CpG and double-stranded RNA trigger human NK cells by Toll-like receptors: induction of cytokine release and cytotoxicity against tumors and dendritic cells.* Proc Natl Acad Sci U S A, 2004. **101**(27): p. 10116-21.
17. Kulka, M., et al., *Activation of mast cells by double-stranded RNA: evidence for activation through Toll-like receptor 3.* J Allergy Clin Immunol, 2004. **114**(1): p. 174-82.
18. Matsushima, H., et al., *TLR3-, TLR7-, and TLR9-mediated production of proinflammatory cytokines and chemokines from murine connective tissue type skin-derived mast cells but not from bone marrow-derived mast cells.* J Immunol, 2004. **173**(1): p. 531-41.
19. Matsumoto, M., et al., *Establishment of a monoclonal antibody against human Toll-like receptor 3 that blocks double-stranded RNA-mediated signaling.* Biochem Biophys Res Commun, 2002. **293**(5): p. 1364-9.
20. Kaiser, W.J., J.L. Kaufman, and M.K. Offermann, *IFN-alpha sensitizes human umbilical vein endothelial cells to apoptosis induced by double-stranded RNA.* J Immunol, 2004. **172**(3): p. 1699-710.
21. Akira, S., *TLR signaling.* Curr Top Microbiol Immunol, 2006. **311**: p. 1-16.
22. Sen, G.C. and S.N. Sarkar, *Transcriptional signaling by double-stranded RNA: role of TLR3.* Cytokine Growth Factor Rev, 2005. **16**(1): p. 1-14.
23. Hasan, U., et al., *Human TLR10 is a functional receptor, expressed by B cells and plasmacytoid dendritic cells, which activates gene transcription through MyD88.* J Immunol, 2005. **174**(5): p. 2942-50.
24. Vercammen, E., J. Staal, and R. Beyaert, *Sensing of viral infection and activation of innate immunity by toll-like receptor 3.* Clin Microbiol Rev, 2008. **21**(1): p. 13-25.
25. Santoro, M.G., et al., *The relationship between the antiviral action of interferon and prostaglandins in virus-infected murine cells.* Biochem Biophys Res Commun, 1983. **116**(2): p. 442-8.
26. Shaw, A.S. and E.L. Filbert, *Scaffold proteins and immune-cell signalling.* Nat Rev Immunol, 2009. **9**(1): p. 47-56.
27. Gatot, J.S., et al., *Lipopolysaccharide-mediated interferon regulatory factor activation involves TBK1-IKKepsilon-dependent Lys(63)-linked polyubiquitination and phosphorylation of TANK/I-TRAF.* J Biol Chem, 2007. **282**(43): p. 31131-46.
28. Sasai, M., M. Matsumoto, and T. Seya, *The kinase complex responsible for IRF-3-mediated IFN-beta production in myeloid dendritic cells (mDC).* J Biochem, 2006. **139**(2): p. 171-5.
29. Sasai, M., et al., *Cutting Edge: NF-kappaB-activating kinase-associated protein 1 participates in TLR3/Toll-IL-1 homology domain-containing adapter molecule-1-mediated IFN regulatory factor 3 activation.* J Immunol, 2005. **174**(1): p. 27-30.

30. Ryzhakov, G. and F. Randow, *SINTBAD, a novel component of innate antiviral immunity, shares a TBK1-binding domain with NAP1 and TANK.* EMBO J, 2007. **26**(13): p. 3180-90.
31. Huang, J., et al., *SIKE is an IKK epsilon/TBK1-associated suppressor of TLR3- and virus-triggered IRF-3 activation pathways.* EMBO J, 2005. **24**(23): p. 4018-28.
32. Saitoh, T., et al., *A20 is a negative regulator of IFN regulatory factor 3 signaling.* J Immunol, 2005. **174**(3): p. 1507-12.
33. You, M., D.H. Yu, and G.S. Feng, *Shp-2 tyrosine phosphatase functions as a negative regulator of the interferon-stimulated Jak/STAT pathway.* Mol Cell Biol, 1999. **19**(3): p. 2416-24.
34. Schroder, K., et al., *Differential effects of CpG DNA on IFN-beta induction and STAT1 activation in murine macrophages versus dendritic cells: alternatively activated STAT1 negatively regulates TLR signaling in macrophages.* J Immunol, 2007. **179**(6): p. 3495-503.
35. An, H., et al., *SHP-2 phosphatase negatively regulates the TRIF adaptor protein-dependent type I interferon and proinflammatory cytokine production.* Immunity, 2006. **25**(6): p. 919-28.
36. Morrison, B.H., et al., *Apo2L/TRAIL induction and nuclear translocation of inositol hexakisphosphate kinase 2 during IFN-beta-induced apoptosis in ovarian carcinoma.* Biochem J, 2005. **385**(Pt 2): p. 595-603.
37. Robinson, J.H., et al., *Transition probability and the hormonal and density-dependent regulation of cell proliferation.* Nature, 1976. **262**(5566): p. 298-300.
38. Arnaud, P., *[The interferons: pharmacology, mechanism of action, tolerance and side effects].* Rev Med Interne, 2002. **23 Suppl 4**: p. 449s-458s.
39. Markman, M., et al., *Phase 2 trial of interferon-beta as second-line treatment of ovarian cancer, fallopian tube cancer, or primary carcinoma of the peritoneum.* Oncology, 2004. **66**(5): p. 343-6.
40. Boehm, J.S., et al., *Integrative genomic approaches identify IKBKE as a breast cancer oncogene.* Cell, 2007. **129**(6): p. 1065-79.
41. Matsuoka, S., et al., *ATM and ATR substrate analysis reveals extensive protein networks responsive to DNA damage.* Science, 2007. **316**(5828): p. 1160-6.
42. Ni, C.Z., et al., *Molecular basis for CD40 signaling mediated by TRAF3.* Proc Natl Acad Sci U S A, 2000. **97**(19): p. 10395-9.
43. Li, P., et al., *Cytochrome c and dATP-dependent formation of Apaf-1/caspase-9 complex initiates an apoptotic protease cascade.* Cell, 1997. **91**(4): p. 479-89.
44. Martinon, F. and J. Tschopp, *Inflammatory caspases: linking an intracellular innate immune system to autoinflammatory diseases.* Cell, 2004. **117**(5): p. 561-74.
45. Motshwene, P.G., et al., *An oligomeric signaling platform formed by the Toll-like receptor signal transducers MyD88 and IRAK-4.* J Biol Chem, 2009. **284**(37): p. 25404-11.

46. Dam, J., et al., *Sedimentation velocity analysis of heterogeneous protein-protein interactions: Lamm equation modeling and sedimentation coefficient distributions c(s).* Biophys J, 2005. **89**(1): p. 619-34.

# VITA

Jonathan L. Forbes was born in Syracuse, New York, U.S.A. in 1984. Upon graduating from Jamesville Dewitt High School, he attended the State University of New York at Buffalo, graduating with a Bachelor of Arts in Biological Sciences in 2008. His current publications include "*Identification of an antiparallel coiled-coil/loop domain required for ligand binding by the Borrelia hermsii FhbA protein: additional evidence for the role of FhbA in the host-pathogen interaction*" in the journal, Infection and Immunity (2008). He received his Master of Science degree in Biochemistry and Molecular Biology from Virginia Commonwealth University in May 2010. He plans to pursue a career in the medicines and medical research.